

Mechanisms of proton-proton inelastic cross-section growth in multi-peripheral model within the framework of perturbation theory. Part 1

I.V. Sharf,¹ G.O. Sokhrannyi,¹ A.V. Tykhonov,^{1,2} K.V. Yatkin,¹ N.A. Podolyan,¹ M.A. Deliyergiyev,^{1,2} and V.D. Rusov^{1,3, a)}

¹⁾ *Odessa National Polytechnic University, Shevchenko av. 1, Odessa, 65044, Ukraine.*

²⁾ *Department of Experimental Particle Physics, Jozef Stefan Institute, Jamova 39, SI-1000 Ljubljana, Slovenia.*

³⁾ *Department of Mathematics, Bielefeld University, Universitätsstrasse 25, 33615 Bielefeld, Germany.*

(Dated: 26 January 2020)

We demonstrate a possibility of computation of inelastic scattering cross-section in a multi-peripheral model by application of the Laplace method to multidimensional integral over the domain of physical process. Founded the constrained maximum point of scattering cross-section integral under condition of the energy-momentum conservation. The integrand is substituted for an expression of Gaussian type in the neighborhood of this point. It made possible to compute this integral numerically. The paper has two parts. The hunting procedure of the constrained maximum point is considered and the properties of this maximum point are discussed in the given part of the paper. It is shown that virtuality of all internal lines of the “comb” diagram reduced at the constrained maximum point with energy growth. In the second part of the paper we give some the arguments in favor of consideration of the mechanism of virtuality reduction as the mechanism of the total hadron scattering cross-section growth, which is not taken into account within the framework of Regge theory.

Keywords: inelastic scattering cross-section, total scattering cross-section, Laplace method, virtuality, multi-peripheral model, Regge theory

I. INTRODUCTION

Despite the fact the multi-peripheral model [1] has been used for description of hadron scattering for a long time, formal difficulties, which appear in calculating of inelastic scattering cross-section, in our opinion, are not overcome until now. These difficulties are caused by the fact that inelastic scattering cross-section with production of a given number of secondary particles in the finite state Fig.1 is described by the multidimensional integral of scattering amplitude squared modulus over the phase volume of finite state:

$$\sigma_n = \frac{1}{4n!I} \int \frac{d\vec{P}_3}{2P_{30}(2\pi)^3} \frac{d\vec{P}_4}{2P_{40}(2\pi)^3} \prod_{k=1}^n \frac{d\vec{p}_k}{2p_{0k}(2\pi)^3} \times \Phi \delta^{(4)} \left(P_3 + P_4 + \sum_{k=1}^n p_k - P_1 - P_2 \right) \quad (1)$$

with

$$I = \sqrt{(P_1 P_2)^2 - (M_1 M_2)^2} \quad (2a)$$

$$\Phi = |T(n, p_1, p_2, \dots, p_n, P_1, P_2, P_3, P_4)|^2 \quad (2b)$$

where M_1 and M_2 are the masses of colliding particles with four-momentums P_1 and P_2 ;

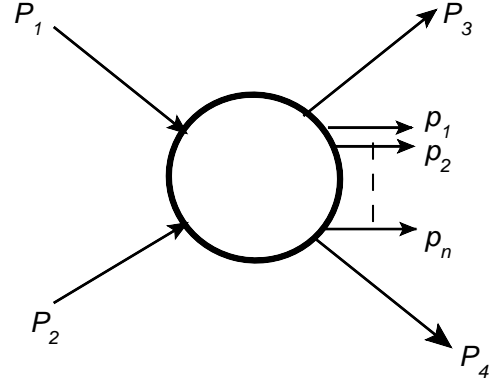


FIG. 1. A general view of an inelastic scattering diagram.

$T(n, p_1, p_2, \dots, p_n, P_1, P_2, P_3, P_4)$ is scattering amplitude corresponding to inelastic process shown in Fig.1; $\delta^{(4)}$ is a four-dimensional delta function describing the conservation laws of energy and three momentum components in this process. Here it is also assumed that particles with four-momentums P_3 and P_4 are the same sorts as P_1 and P_2 , respectively, and n secondary particles with four-momentums p_1, p_2, \dots, p_n are identical. Since scattering amplitude is, in general, not a product of functions of some variables, and also due to the complexity of integration domain, the multidimensional integral in Eq.1 is not a product of smaller-dimensional ones. In considered inelastic process this domain of phase space of finite state particles is determined by the energy-momentum

^{a)} Electronic mail: siiis@te.net.ua

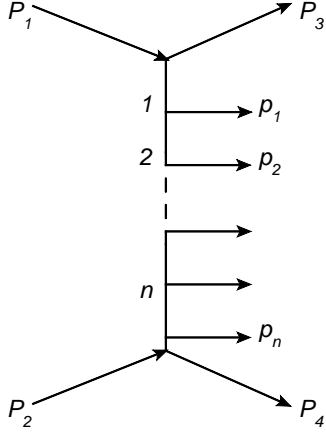


FIG. 2. An elementary inelastic scattering diagram in the multi-peripheral model (“the comb”).

conservation law. As a result, the integration limits for one variable depend on the values of others. In order to overcome these difficulties one usually deals with the multi-Regge kinematics [2–10].

In our approach we will adopt well-known Laplace method [11] for scattering amplitude, which represented by set of multi-peripheral diagrams Fig.2 within the framework of the perturbation theory in order to overcome these difficulties. The essence of this method consists in finding the constrained maximum point of scattering amplitude squared modulus in Eq.1 under four conditions imposed by $\delta^{(4)}$ -function of Eq.1. Then, expressing the scattering amplitude squared modulus as $|T|^2 = \exp(\ln(|T|^2))$, it is possible to expand the exponent in Taylor series in the neighborhood of constrained maximum point, coming to nothing more than quadratic items. After that we obtain Gaussian integral, whose calculation is reduced to computation of matrix determinant of second derivatives with respect to $\ln(|T|^2)$. Now let us consider solution of the listed above problems step by step.

II. CONSIDERATION OF THE SCATTERING AMPLITUDE SYMMETRY PROPERTIES

At first we examine some simplifications, which is possible to make before hunting for the solution of constrained maximum problem. According to Feynman diagram technique, the expression for scattering amplitude, which corresponds to a diagram Fig.2 has form:

$$\begin{aligned}
 T(n, P_3, P_4, p_1, p_2, \dots, p_n, P_1, P_2) &= \left(-ig(2\pi)^4\right)^2 \\
 &\times \left(-i\lambda(2\pi)^4\right)^n \left(\frac{-i}{(2\pi)^4}\right)^{n+1} \\
 &\times A(n, P_3, P_4, p_1, p_2, \dots, p_n, P_1, P_2)
 \end{aligned} \quad (3)$$

with

$$\begin{aligned}
 A(n, P_3, P_4, p_1, p_2, \dots, p_n, P_1, P_2) &= \\
 &= \frac{1}{m^2 - (P_1 - P_3)^2 - i\varepsilon} \\
 &\times \frac{1}{m^2 - (P_1 - P_3 - p_1)^2 - i\varepsilon} \\
 &\times \frac{1}{m^2 - (P_1 - P_3 - p_1 - p_2)^2 - i\varepsilon} \dots \dots \dots \\
 &\times \frac{1}{m^2 - (P_1 - P_3 - p_1 - p_2 - \dots - p_{n-1})^2 - i\varepsilon} \\
 &\times \frac{1}{m^2 - (P_1 - P_3 - p_1 - p_2 - \dots - p_{n-1} - p_n)^2 - i\varepsilon}
 \end{aligned} \quad (4)$$

where g is a coupling constant in the outermost vertices of the diagram; λ is a coupling constant in all other vertices; m is the mass of virtual particle field and also secondary particles. As in the original version of multi-peripheral model [1], pions are taken both as virtual and secondary particles. It was assumed that the particle masses with four-momentums P_1, P_2, P_3, P_4 are equal, i.e., $M_1 = M_2 = M_3 = M_4 = M$. The proton mass was taken as M . Note that the concrete choice of numerical value of mass M has no importance for the results presented in the paper.

As it was noted in [2], for the most ratios of particle masses in the initial and final state, the virtual particles four-momentums on the diagram of Fig.2 are space-like, i.e., their scalar squares are negative in Minkowski space. The negativity of scalar squares of virtual four-momentums at the given mass configuration $M_1 = M_2 = M_3 = M_4 = M$ is easy to prove (see Appendix.A).

Since the virtual particle squared four-momentums $(P_1 - P_3)^2, (P_1 - P_3 - p_1)^2, (P_1 - P_3 - p_1 - p_2 - \dots - p_n)^2$ are negative at the physical values of four-momentums of particles in the finite state, denominators in Eq.1 do not equal to zero nowhere in the physical region. Therefore it is possible to reduce $i\varepsilon$ to zero before all calculations.

Due to negativity of virtual particle squared four-momentums the magnitude Eq.4 is real and positive. Therefore the search of the constrained maximum point of scattering amplitude squared modulus reduces to the search of the constrained maximum point of function Eq.4. Hereinafter we'll refer the expression Eq.4 as well as Eq.3, which differs from it by constant factor, as scattering amplitude, for short.

Let us examine Eq.4 in c.m.s. of colliding particles P_1 and P_2 . In such a frame of reference the initial and final states have some symmetry, which is possible to use for solving the constrained maximum problem. In particular, the consideration of symmetries makes it possible to reduce the search of the constrained maximum of scattering amplitude to the search of the maximum of its restriction on a certain subset of physical process domain shown in Fig.2. This restriction is the function

of substantially smaller number of independent variables than the initial amplitude.

For the further discussion of these symmetries and related simplifications, it would be convenient at first to take into account the conservation laws, expressing the scattering amplitude as a function of independent variables only. After decomposition of the three-dimensional particle momentums in c.m.s. frame to components, which are parallel $p_{k\parallel}$ and orthogonal $\vec{k}_{k\perp}$ to collision axis, and let's name them longitudinal and transversal momentums, respectively.

Energy of each particles in the finite state can be expressed by their momentum using the mass shell conditions, having $n + 2$ particles in finite state Fig.2, that give us $3(n + 2)$ momentum components of these particles. Since we are looking for a constrained extremum, it is necessary to take into account four relations, which express an energy-momentum conservation law. It will result in the fact that amplitude Eq.4 can be represented as a function of $3n + 2$ independent variables. The first $3n$ variables we choose are longitudinal and transverse components of momentums $\vec{p}_1, \vec{p}_2, \dots, \vec{p}_n$ of particles produced along the “comb” in Fig.2. The other two variables are the transverse components of momentum $\vec{P}_{3\perp}$.

If z -axis coincides with momentum direction \vec{P}_1 in c.m.s. and x and y axes are the coordinate axes in the plane of transverse momentums, the conservation laws look like

$$\begin{aligned} P_{30} + P_{40} &= \sqrt{s} - (p_{10} + p_{20} + \dots + p_{n0}) \\ P_{3\parallel} + P_{4\parallel} &= -(p_{1\parallel} + p_{2\parallel} + \dots + p_{n\parallel}) \\ P_{4\perp x} &= -(p_{1\perp x} + p_{2\perp x} + \dots + p_{n\perp x} + P_{3\perp x}) \\ P_{4\perp y} &= -(p_{1\perp y} + p_{2\perp y} + \dots + p_{n\perp y} + P_{4\perp y}) \end{aligned} \quad (5)$$

with

$$\begin{aligned} s &= (P_1 + P_2)^2 \\ p_{k0} &= \sqrt{m^2 + (p_{k\parallel})^2 + (p_{k\perp x})^2 + (p_{k\perp y})^2} \\ P_{30} &= \sqrt{M^2 + (P_{3\parallel})^2 + (P_{3\perp x})^2 + (P_{3\perp y})^2} \\ P_{40} &= \sqrt{M^2 + (P_{4\parallel})^2 + (P_{4\perp x})^2 + (P_{4\perp y})^2} \end{aligned} \quad (6)$$

Let's enter the following denotations:

$$\begin{aligned} E_p &\equiv \sqrt{s} - (p_{10} + p_{20} + \dots + p_{n0}) \\ P_{\parallel p} &\equiv -(p_{1\parallel} + p_{2\parallel} + \dots + p_{n\parallel}) \\ P_{px} &\equiv -(p_{1\perp x} + p_{2\perp x} + \dots + p_{n\perp x}) \\ P_{py} &\equiv -(p_{1\perp y} + p_{2\perp y} + \dots + p_{n\perp y}) \end{aligned} \quad (7)$$

Then solving the system Eq.5 for the unknown $P_{3\parallel}, P_{4\parallel}, P_{4\perp x}, P_{4\perp y}$, we have:

$$\begin{aligned} P_{3\parallel} &= \frac{E_a}{2E_b} \left(-P_{\parallel p} \pm E_p \sqrt{1 - \frac{4(M^2 + (\vec{P}_{3\perp})^2)E_b}{(E_a)^2}} \right) \\ P_{4\parallel} &= \frac{E_a}{2E_b} \left(-P_{\parallel p} \mp E_p \sqrt{1 - \frac{4(M^2 + (\vec{P}_{3\perp})^2)E_b}{(E_a)^2}} \right) \end{aligned} \quad (8)$$

where

$$\vec{P}_{p\perp} = (P_{px}, P_{py}) \quad (9a)$$

$$E_a = E_p^2 - P_{\parallel p}^2 - \vec{P}_{p\perp}^2 - 2(\vec{P}_{p\perp} \cdot \vec{P}_{3\perp}) \quad (9b)$$

$$E_b = (E_p^2 - P_{\parallel p}^2) \quad (9c)$$

We will discuss the choice of sign in Eq.8 further in the paper. Note that the value of $P_{3\parallel}$ will not change, if we change the signs of all transversal momentums in Eq.8 simultaneously.

Substituting $P_{3\parallel}$ from Eq.8 to Eq.6, and resulting P_{30} from Eq.6 into Eq.4, give us the scattering amplitude as a function of independent variables, for which the conservation laws of all components of energy-momentum four-vector are taken into account. Below, referring to Eq.4, we assume that these substitutions have already been done. Taking into account this fact, we can define the amplitude Eq.4 as

$$A(n, \vec{P}_{3\perp}, \vec{p}_{1\perp}, \vec{p}_{2\perp}, \dots, \vec{p}_{n\perp}, p_{1\parallel}, p_{2\parallel}, \dots, p_{n\parallel}) \quad (10)$$

enumerating only independent variables in the argument list. When the scattering amplitude will be expressed in terms of independent variables only, it is possible to find the ordinary extremum, but not constrained extremum.

Now let us examine symmetries of the scattering amplitude in c.m.s. Obviously, the system has a symmetry under rotations around the collision axis, it means that there is no preferred direction in the plane orthogonal to collision axis. Hence, if the scattering amplitude has the constrained maximum point, it must be achieved at zero values of the particle momentums components in finite state transversal to collision axis. Otherwise these momentums must be somehow directed in the plane of transversal momentums, while all directions are equivalent in this plane.

To show more formally previous conclusion we use an explicit form of amplitude Eq.4, which transforms to itself, when the signs in front of all transversal momentums are changed:

$$\begin{aligned} &A(n, \vec{P}_{3\perp}, \vec{p}_{1\perp}, \vec{p}_{2\perp}, \dots, \vec{p}_{n\perp}, p_{1\parallel}, p_{2\parallel}, \dots, p_{n\parallel}) \\ &= A(n, -\vec{P}_{3\perp}, -\vec{p}_{1\perp}, -\vec{p}_{2\perp}, \dots, -\vec{p}_{n\perp}, p_{1\parallel}, p_{2\parallel}, \dots, p_{n\parallel}) \end{aligned} \quad (11)$$

Take derivative from Eq.11 with respect to any of transversal momentum arguments and after that assuming all transversal momentums equal to zero, we obtain that all partial derivatives with respect to transverse momentum arguments are equal to zero if this arguments are equal to zero.

Thus, for the further search of the constrained maximum we can limit ourselves to reduction of the scattering amplitude on a subset of the values of its independent arguments, which corresponds to zero values of transversal momentums of all particles in finite

state. This reduction is a function of longitudinal components of momentum $p_{1\parallel}, p_{2\parallel}, \dots, p_{n\parallel}$, which we designate as $A_{\parallel}(n, p_{1\parallel}, p_{2\parallel}, \dots, p_{n\parallel})$ and from Eq.4 we get:

$$\begin{aligned} A_{\parallel}(n, p_{1\parallel}, p_{2\parallel}, \dots, p_{n\parallel}) &= \\ &= \left(m^2 - (P_{10} - P_{30})^2 + (P_{1\parallel} - P_{3\parallel})^2 \right)^{-1} \\ &\times \prod_{l=1}^n (m^2 - \alpha_l^2 + \beta_l^2)^{-1} \end{aligned} \quad (12)$$

where

$$\alpha_l = P_{10} - P_{30} - \sum_{k=1}^l p_{k0} \quad (13a)$$

$$\beta_l = P_{1\parallel} - P_{3\parallel} - \sum_{k=1}^l p_{k\parallel} \quad (13b)$$

$$p_{k0} = \sqrt{m^2 + (p_{k\parallel})^2} \quad (13c)$$

$$P_{30} = \sqrt{M^2 + (P_{3\parallel})^2} \quad (13d)$$

At the same time, assuming that all transversal momentums equal to zero, we have from Eq.8:

$$\begin{aligned} P_{3\parallel} &= \frac{1}{2} \left(P_{\parallel p} \pm E_p \sqrt{1 - \frac{4M^2}{(E_p)^2 - (P_{\parallel p})^2}} \right) \\ P_{4\parallel} &= \frac{1}{2} \left(P_{\parallel p} \mp E_p \sqrt{1 - \frac{4M^2}{(E_p)^2 - (P_{\parallel p})^2}} \right) \end{aligned} \quad (14)$$

Moreover, we have in c.m.s. $P_{10} = \sqrt{s}/2$ and $P_{1\parallel} = \sqrt{s/4 - M^2}$, where s is determined in Eq.6.

For the further analysis it is convenient to switch from longitudinal momentums of secondary particles to rapidities y_k , defined by following relation:

$$p_{k\parallel} = m \cdot sh(y_k), \quad k = 1, 2, \dots, n \quad (15)$$

The function A_{\parallel} can be written as $A_{\parallel} = A_{\parallel}(n, y_1, y_2, \dots, y_n)$. The initial state in c.m.s is symmetric with respect to changes in positive direction of collision axis. In addition, those type of diagrams of presented in Fig.2 have an axis of symmetry shown in Fig.3 for the case of even number Fig.3(a) and for the case of odd number Fig.3(b) of secondary particles.

From the explicit expression for amplitude Eq.12 can be shown that this expression will transform to itself, if we place instead the rapidity of every particle, the rapidity of particle symmetrically arrangement along the axis of symmetry Fig.3 and at the same time change the rapidity sign. Other words, if we change the variables for even number of particles

$$\begin{aligned} y_1 &\rightarrow -y_n, y_2 \rightarrow -y_{n-1}, \dots, y_{\frac{n}{2}} \rightarrow -y_{\frac{n}{2}+1}, \\ y_{\frac{n}{2}+1} &\rightarrow -y_{\frac{n}{2}}, \dots, y_n \rightarrow -y_1 \end{aligned} \quad (16)$$

the expression of restriction amplitude $A_{\parallel}(n, y_{1\parallel}, y_{2\parallel}, \dots, y_{n\parallel})$ will transform to itself. In

case of odd number of particles the transformation similar to Eq.16, but instead of the rapidity $y_{\frac{n-1}{2}+1}$ which forms the axis of symmetry in Fig.3, must be substituted $-y_{\frac{n-1}{2}+1}$ into the expression for the amplitude. The examined features of function $A_{\parallel}(n, y_{1\parallel}, y_{2\parallel}, \dots, y_{n\parallel})$ can be expressed in the following symmetry relations for even number n of secondary particles :

$$\begin{aligned} A_{\parallel}(n, y_1, y_2, \dots, y_{\frac{n}{2}}, y_{\frac{n}{2}+1}, \dots, y_n) \\ = A_{\parallel}(n, -y_n, -y_{n-1}, \dots, -y_{\frac{n}{2}+1}, -y_{\frac{n}{2}}, \dots, -y_1) \end{aligned} \quad (17)$$

and for odd number n of secondary particles, respectively:

$$\begin{aligned} A_{\parallel}(n, y_1, y_2, \dots, y_{\frac{n-1}{2}}, y_{\frac{n-1}{2}+1}, y_{\frac{n-1}{2}+2}, \dots, y_{n-1}, y_n) \\ = A_{\parallel}(n, -y_n, -y_{n-1}, \dots, -y_{\frac{n-1}{2}+1}, -y_{\frac{n-1}{2}}, \dots, -y_2, -y_1) \end{aligned} \quad (18)$$

Proof of symmetry relations Eq.17 is given in Appendix.B.

Now let us switch to new variables for even number of n

$$\begin{aligned} y_1^+ &= \frac{y_1 + y_n}{2}, y_2^+ = \frac{y_2 + y_{n-1}}{2}, \dots, y_{\frac{n}{2}}^+ = \frac{y_{\frac{n}{2}} + y_{\frac{n}{2}+1}}{2} \\ y_1^- &= \frac{y_1 - y_n}{2}, y_2^- = \frac{y_2 - y_{n-1}}{2}, \dots, y_{\frac{n}{2}}^- = \frac{y_{\frac{n}{2}} - y_{\frac{n}{2}+1}}{2} \end{aligned} \quad (19)$$

and for odd number of n

$$\begin{aligned} y_1^+ &= \frac{y_1 + y_n}{2}, y_2^+ = \frac{y_2 + y_{n-1}}{2}, \dots, y_{\frac{n-1}{2}}^+ = \frac{y_{\frac{n-1}{2}} + y_{\frac{n-1}{2}+2}}{2}, \\ y_{\frac{n-1}{2}+1}^+ &= y_{\frac{n-1}{2}+1} \\ y_1^- &= \frac{y_1 - y_n}{2}, y_2^- = \frac{y_2 - y_{n-1}}{2}, \dots, y_{\frac{n-1}{2}}^- = \frac{y_{\frac{n-1}{2}} - y_{\frac{n-1}{2}+2}}{2} \end{aligned} \quad (20)$$

In these variables, the symmetry relation Eq.17 becomes

$$\begin{aligned} A_{\parallel}(n, y_1^+, y_2^+, \dots, y_{\frac{n}{2}}^+, y_1^-, y_2^-, \dots, y_{\frac{n}{2}}^-) \\ = A_{\parallel}(n, -y_1^+, -y_2^+, \dots, -y_{\frac{n}{2}}^+, y_1^-, y_2^-, \dots, y_{\frac{n}{2}}^-) \end{aligned} \quad (21)$$

and relation Eq.18 becomes

$$\begin{aligned} A_{\parallel}(n, y_1^+, y_2^+, \dots, y_{\frac{n-1}{2}+1}^+, y_1^-, y_2^-, \dots, y_{\frac{n-1}{2}}^-) \\ = A_{\parallel}(n, -y_1^+, -y_2^+, \dots, -y_{\frac{n-1}{2}+1}^+, y_1^-, y_2^-, \dots, y_{\frac{n-1}{2}}^-) \end{aligned} \quad (22)$$

Computing step by step the partial derivative of function Eq.22 with respect to variables $y_1^+, y_2^+, \dots, y_{n/2}^+$, we obtain

$$\begin{aligned} \frac{\partial}{\partial y_k^+} A_{\parallel}(n, y_1^+, y_2^+, \dots, y_{\frac{n}{2}}^+, y_1^-, y_2^-, \dots, y_{\frac{n}{2}}^-) \\ = -\frac{\partial}{\partial y_k^+} A_{\parallel}(n, -y_1^+, -y_2^+, \dots, -y_{\frac{n}{2}}^+, y_1^-, y_2^-, \dots, y_{\frac{n}{2}}^-) \end{aligned} \quad (23)$$

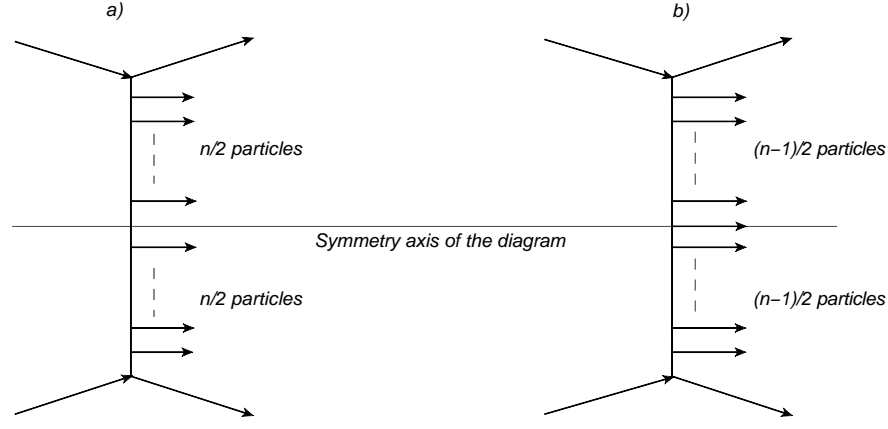


FIG. 3. An elementary inelastic scattering diagram in the multi-peripheral model with even (a) and with odd (b) number of particles on the “comb” and its symmetry axis.

where $k = 1, 2, \dots, \frac{n}{2}$.

It follows from relation Eq.23 for zero values of y_k^+ the derivatives of the function $A_{\parallel} \left(n, y_1^+, y_2^+, \dots, y_{\frac{n}{2}}^+, y_1^-, y_2^-, \dots, y_{\frac{n}{2}-1}^-, y_{\frac{n}{2}}^- \right)$ vanish. In the same way it can be shown that in case of odd number n of particles that for zero values of y_k^+ the derivatives of scattering amplitude $A_{\parallel} \left(n, y_1^+, y_2^+, \dots, y_{\frac{n-1}{2}+1}^+, y_1^-, y_2^-, \dots, y_{\frac{n-1}{2}}^- \right)$ also vanishes.

This shows that for the extremum search we can consider a further reduction of the scattering amplitude on a subset of zero values of variables y_k^+ . By virtue of Eqs.20 - 21 on this subset we have $y_k^- = y_k$, $k = 1, 2, \dots, \frac{n-1}{2}$ at even n and $y_k^- = y_k$, $k = 1, 2, \dots, \frac{n}{2}$ at odd n . Designating this reduction as A_0 we obtain at even n :

$$\begin{aligned} A_0(n, y_1, y_2, \dots, y_{\frac{n}{2}}) \\ = A_{\parallel}(n, y_1, y_2, \dots, y_{\frac{n}{2}}, -y_{\frac{n}{2}-1}, \dots, -y_2, -y_1) \end{aligned} \quad (24)$$

and at odd n

$$\begin{aligned} A_0 \left(n, y_1, y_2, \dots, y_{\frac{n-1}{2}} \right) \\ = A_{\parallel} \left(n, y_1, y_2, \dots, y_{\frac{n-1}{2}+1} = 0, -y_{\frac{n-1}{2}+1}, -y_{\frac{n-1}{2}}, \dots, -y_1 \right) \end{aligned} \quad (25)$$

If we now examine the formula Eq.12 on subset, where reduction A_0 is considered, we will have $P_p = 0$ by virtue of Eq.7. And therefore instead of Eq.14 we have the following expressions:

$$P_{3\parallel} = \frac{E_p}{2} \sqrt{1 - \frac{4M^2}{(E_p)^2}}; P_{4\parallel} = \frac{-E_p}{2} \sqrt{1 - \frac{4M^2}{(E_p)^2}} \quad (26)$$

or

$$P_{3\parallel} = \frac{-E_p}{2} \sqrt{1 - \frac{4M^2}{(E_p)^2}}; P_{4\parallel} = \frac{E_p}{2} \sqrt{1 - \frac{4M^2}{(E_p)^2}} \quad (27)$$

Let us take into account that if we decompose all scalar square terms in denominators of Eq.4 they will include the following difference $P_{1\parallel} - P_{3\parallel} = \sqrt{s/4 - M^2} - P_{3\parallel}$ and negative Eq.27, chosen as the $P_{3\parallel}$ in the end will give us greater value in the denominator than in the choice of Eq.26. Therefore it is naturally to suppose that the main contribution to cross-section Eq.1 gives the range of constrained maximum point determined by the scattering amplitude, where $P_{3\parallel}$ and $P_{4\parallel}$ are given by Eq.26, but not by Eq.27. Hence, considering the expression Eq.24 and Eq.25 for the reduction of the scattering amplitude at zero transverse momentum region, and performing further transformations, we assume that $P_{3\parallel}$ and related with it $P_{30} = \sqrt{M^2 + (P_{3\parallel})^2}$ are expressed in terms of the longitudinal momenta of secondary particles by the relation Eq.26.

After we move on to the appropriate amplitude reduction A_0 both in case of diagrams with even and odd number of particles we obtain function of particles rapidities located above the axis of symmetry in the diagram. The considered features of symmetry make it possible to simplify the energy parametrization of virtual particles, to which correspond the transversal lines located above axis of symmetry of diagrams in Fig 3.

Applying symmetry relation and conservation of energy, it follows that on subset, on which the considered amplitude reduction A_0 is defined, the energy corresponding to the line connecting $n/2$ and $n/2 + 1$ vertices of the diagram in Fig.2 is equal to zero in case of even number of particles at any values of independent variables (on which A_0 depends). Similarly, for an odd number of particles the energy transferred along the line, which joins $(n-1)/2$ and $(n-1)/2 + 1$ vertices, is equal to $m/2$. The corresponding proof is given in Appendix.C.

Taking into account these results, reduction of A_0 for the diagram in Fig.2 with even number of particles can be written in the form, which is convenient for the further

numerical and analytical calculations:

$$\begin{aligned}
A_0(n, y_1, y_2, \dots, y_{\frac{n}{2}}) &= \left(m^2 - \left(\sum_{k=1}^{\frac{n}{2}} E_k \right)^2 + (S_M)^2 \right)^{-2} \\
&\times \prod_{j=2}^{\frac{n}{2}} \left(m^2 - \left(\sum_{k=j}^{\frac{n}{2}} E_k \right)^2 + \left(S_M - \sum_{k=1}^{j-1} p_{k\parallel} \right)^2 \right)^{-2} \\
&\times \left(m^2 + \left(S_M - \sum_{k=1}^{\frac{n}{2}} p_{k\parallel} \right)^2 \right)^{-1}
\end{aligned} \quad (28)$$

where

$$S_M = \sqrt{s/4 - M^2} - P_{3\parallel} \quad (29a)$$

$$E_k = m \cdot ch(y_k) \quad (29b)$$

$$p_{k\parallel} = m \cdot sh(y_k) \quad (29c)$$

The similar expression in case of odd number of particles in comb looks like:

$$\begin{aligned}
A_0(n, y_1, y_2, \dots, y_{\frac{n-1}{2}}) &= \left(m^2 - \left(\frac{m}{2} + \sum_{k=1}^{\frac{n-1}{2}} E_k \right)^2 + (S_M)^2 \right)^{-2} \\
&\times \prod_{j=2}^{\frac{n-1}{2}} \left(m^2 - \left(\frac{m}{2} + \sum_{k=j}^{\frac{n-1}{2}} E_k \right)^2 + \left(S_M - \sum_{k=1}^{j-1} p_{k\parallel} \right)^2 \right)^{-2} \\
&\times \left(m^2 - \left(\frac{m}{2} \right)^2 + \left(S_M - \sum_{k=1}^{\frac{n-1}{2}} p_{k\parallel} \right)^2 \right)^{-2}
\end{aligned} \quad (30)$$

As it follows from Eqs.28 - 30, it is convenient for the further calculations to make all quantities dimensionless by mass m . In dimensionless form, these relations were used for numerical and analytical solution of the extremum for the reduction of the scattering amplitude A_0 .

III. NUMERICAL SOLVING THE CONSTRAINED MAXIMUM PROBLEM FOR MULTI-PERIPHERAL SCATTERING AMPLITUDE SQUARED MODULE

Numerical solution of the constrained extremum problem was done using Mathcad 2001 [12 and 13]. As it was shown in the previous section, since scattering amplitude corresponding to Fig.2 is real and positive, we can search for amplitude maximum instead the maximum of amplitude squared module. For cases of low values of secondary particles n we search not for the maximum of reduction A_0 , but for the maximum of total amplitude A defined by Eq.4 with allowance for Eq.14 with the choice

TABLE I. A typical output of numerical computation of the maximum point of scattering amplitude corresponding to the diagram presented in Fig.2

index	y	p_x	p_y	P_{3x}	P_{3y}
1	3.33917	0	0	0	0
2	2.75454	0	0	-	-
3	2.15274	0	0	-	-
4	1.54160	0	0	-	-
5	0.92590	0	0	-	-
6	0.30901	0	0	-	-
7	-0.30901	0	0	-	-
8	-0.92590	0	0	-	-
9	-1.54160	0	0	-	-
10	-2.15274	0	0	-	-
11	-2.75454	0	0	-	-
12	-3.33917	0	0	-	-

of positive sign in the front of $P_{3\parallel}$ (in order to transform this expression to Eq.26, when the symmetry properties will be taken into account). These calculations are numerical verification of validity of the discussed above simplifications related to the symmetry properties.

A typical result of such calculation for the case of $n = 12$ and energy $\sqrt{s} = 55$ GeV using Maximize function of Mathcad 2001 is shown in Table.I. As it follows from Table.I, the numerical computation confirms above conclusion that all the transverse momenta must vanish at the maximum point. Note also that the set of rapidities corresponding to the maximum point in Table.I, which are determined by numerical computation, confirms conclusion that the diagrams centered at the axis of symmetry have mutually opposite values in the point of rapidity extremum. Similar results were obtained for different numbers of particles n and energies \sqrt{s} .

Now let us examine properties of the constrained maximum point following from the results of numerical computations. Some typical results are shown on Fig.5 and corresponding to it Table.II.

The column y in Fig.5 contains the rapidities of particles obtained using Maximize procedure (Mathcad) for which scattering amplitude A_0 defined by Eq.28 in the case of even number particles and by Eq.30 in the case of odd number particles has maximum reduction. Moreover, note that the order of numbers in the columns match to the order of arguments in the corresponding function.

For instance, in Fig.4 at $n = 30$ the reduction determined by Eq.28 is the function of 15-en variables $A_0(n = 15, y_1, y_2, \dots, y_{15})$ corresponding to the particles rapidities joined to the upper 15-en vertices of the diagram in Fig.2. The column shown in Table.II contains fifteen numbers, in which the function $A_0(n = 15, y_1, y_2, \dots, y_{15})$ has a maximum and at the same time the first number in the column is the value of y_1 , the second number is the value of y_2 etc.

As it is apparent from Fig.4, there is an interesting feature, which consists in the fact that the maximizing

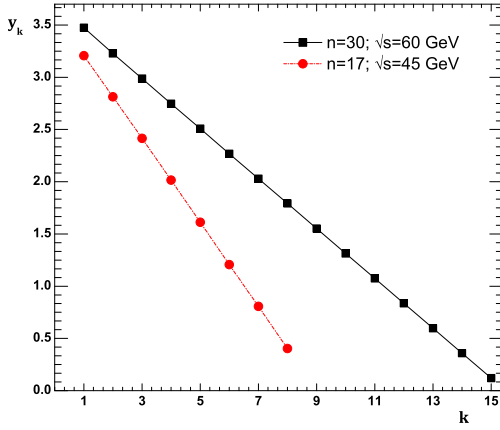


FIG. 4. Rapidity dependence on vertex number in the diagram Fig.2 at the constrained maximum point.

rapidities in the case of even n and in the case of odd n , are approximately equal to the numbers producing arithmetic progression. It is confirmed by the presented dependences in Fig.5. Δy values are approximately equal to each other (see Table.II).

In addition, the proximity of the sequence of y_k column elements to an arithmetic progression follows also from calculations of $\frac{y_k}{y_8}$ and $\frac{y_k}{y_{15}}$ columns, which are constructed by the following principle. If we assume that y_k form an arithmetic progression with difference Δy , in the case of even n we obtain $y_{\frac{n}{2}+1} = y_{\frac{n}{2}} - \Delta y$. On the other hand, from symmetry relations obtained in Section.II we have $y_{\frac{n}{2}+1} = -y_{\frac{n}{2}}$. From these two relations we obtain $y_{\frac{n}{2}} = \frac{\Delta y}{2}$. Then $y_{\frac{n}{2}-1} = y_{\frac{n}{2}} + \Delta y = 3\frac{\Delta y}{2} = 3y_{\frac{n}{2}}$ and in the similar manner $y_{\frac{n}{2}-2} = y_{\frac{n}{2}} + 2\Delta y = 5\frac{\Delta y}{2} = 5y_{\frac{n}{2}}$, etc. Hence, in case of the diagram with even n the rapidity ratios $\frac{y_{\frac{n}{2}-1}}{y_{\frac{n}{2}}}, \frac{y_{\frac{n}{2}-2}}{y_{\frac{n}{2}}}, \dots, \frac{y_1}{y_{\frac{n}{2}}}$ must form the sequence of odd whole numbers. The columns $\frac{y_k}{y_8}$ and $\frac{y_k}{y_{15}}$ contains these ratios constructed by the column elements y_k obtained with the help of Maximize function 12. As seen from Table.II, the column elements $\frac{y_k}{y_8}$ and $\frac{y_k}{y_{15}}$ are really close to odd numbers.

In case of odd n with allowance for $y_{\frac{n-1}{2}+1} = 0$ we have

$$\begin{aligned} y_{\frac{n-1}{2}} &= y_{\frac{n-1}{2}+1} + \Delta y = \Delta y \\ y_{\frac{n-1}{2}-1} &= y_{\frac{n-1}{2}} + \Delta y = 2\Delta y \end{aligned} \quad (31)$$

Then the ratios $\frac{y_{\frac{n-1}{2}}}{y_{\frac{n-1}{2}}}, \frac{y_{\frac{n-1}{2}-1}}{y_{\frac{n-1}{2}}}, \frac{y_{\frac{n-1}{2}-2}}{y_{\frac{n-1}{2}}}$, must produce the sequence of whole numbers 1, 2, And Table.I, where columns $\frac{y_k}{y_8}$ and $\frac{y_k}{y_{15}}$ consist of such ratios, shows that these ratios are really close to the corresponding whole numbers. The similar results are obtained for different numbers of particles n and energies \sqrt{s} .

The analytic form of arithmetic progression at any n and \sqrt{s} will be considered in more detail below the text,

Fig.4 n=30 $\sqrt{s} = 60$ GeV			
index	y_k	$\Delta y = y_k - y_{k+1}$	y_k/y_{15}
1	3.475	0.2461	29.07
2	3.229	0.2417	27.01
3	2.987	0.2399	24.99
4	2.747	0.2392	22.98
5	2.508	0.2389	20.98
6	2.269	0.2387	18.98
7	2.03	0.2387	16.98
8	1.792	0.2387	14.99
9	1.553	0.2387	12.99
10	1.314	0.2388	10.99
11	1.075	0.2389	8.997
12	0.8365	0.2389	6.998
13	0.5976	0.239	4.999
14	0.3586	0.2391	3
15	0.1195	-	1

Fig.4 n=17 $\sqrt{s} = 45$ GeV			
index	y_k	$\Delta y = y_k - y_{k+1}$	y_k/y_8
1	3.207	0.3929	7.951
2	2.814	0.3972	6.977
3	2.416	0.4016	5.992
4	2.015	0.4017	4.996
5	1.613	0.4061	4
6	1.207	0.3992	2.993
7	0.8079	0.4046	2.003
8	0.4033	-	1

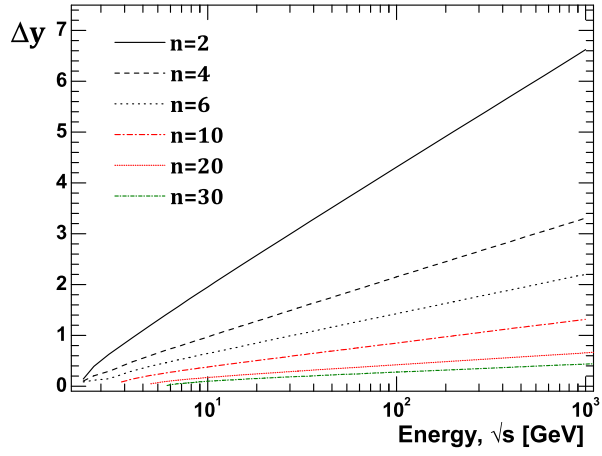
TABLE II. Resulting rapidities obtained using Maximize procedure (Mathcad) for which scattering amplitude A_0 defined by Eq.28 in the case of even number particles and by Eq.30 in the case of odd number particles has maximum reduction. The column Δy contains a difference between every column element and the successor of this column. The last column contains ratios $\frac{y_k}{y_{15}}, k = 1, 2, \dots, 15$ and $\frac{y_k}{y_8}, k = 1, 2, \dots, 8$.

when we will given an analytical solution of the extremum problem for reductions Eq.28 and Eq.30.

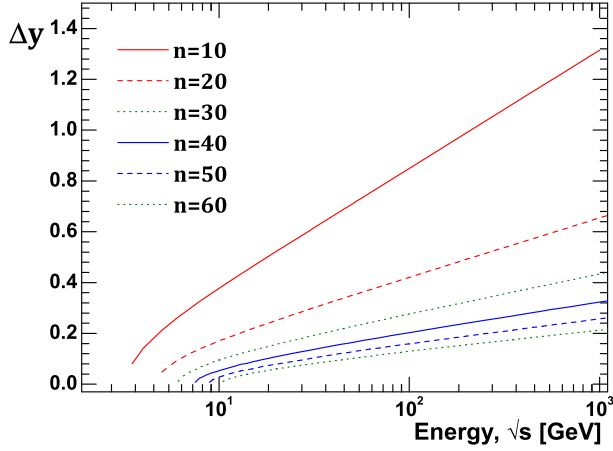
Moreover, the results of numerical computations confirm the well-known multi-peripheral model assumption about particle rapidity ordering, because at the maximum point the particle rapidities monotone increase at movement upward along the diagram in Fig.2.

Besides of these results numerical computation allows to trace several other properties of the extremum point. In particular, if the rapidities in the maximum point form an arithmetic progression, the question arises, how the difference Δy of this arithmetic progression depends on the energy \sqrt{s} and the number of particles n ? Result of numerical computation of the dependence of difference of an arithmetic progression Δy on \sqrt{s} at different numbers of particles on the “comb” Fig.2 are shown in Fig.5. At the same time the arithmetical average of column elements Δy (the similar to shown in Table.II) was used as the value of Δy .

As its obvious from Fig.5, the Δy is a monotonically increasing function of energy \sqrt{s} for a fixed num-



(a)



(b)

FIG. 5. The dependence of rapidity step Δy of an arithmetic progression, which constrainedly maximizing the scattering amplitude, on energy \sqrt{s} for the different numbers n of particles on “the comb”. At high energies this dependence become logarithmic.

ber n of particles. At the same time the dependence $\Delta y(n = \text{const}, \sqrt{s})$ has some energy threshold. It is obvious, that at given n such dependence makes sense only at

$$\sqrt{s} \geq nm + 2M \quad (32)$$

(where \sqrt{s} is not dimensionless by m), that corresponds to the total rest energy of particle in finite state. Note that function $\Delta y(\sqrt{s})$ reaches asymptotic quite quickly. Since Fig.5 has a logarithmic scale on the energy axis, its seen that this asymptotic behavior is characterized by the linear dependence on logarithm of energy normalized to 1 GeV.

Output computation of the dependence of difference of an arithmetic progression Δy on the number of particles for set of energies $\sqrt{s} = 10 \text{ GeV}, 100 \text{ GeV}, 1000 \text{ GeV}$ is presented in Fig.6. From Fig.6 (where dependences $\Delta y(n)$ are given in linear and logarithmic scales)

	10 GeV	\sqrt{s} 100 GeV	1 TeV
$\frac{\ln(\Delta y_4) - \ln(\Delta y_2)}{\ln(4) - \ln(2)}$	-1.009	-1.005	-1.002
$\frac{\ln(\Delta y_6) - \ln(\Delta y_2)}{\ln(6) - \ln(2)}$	-1.011	-1.006	-1.003
$\frac{\ln(\Delta y_{20}) - \ln(\Delta y_2)}{\ln(20) - \ln(2)}$	-1.057	-1.011	-1.002
$\frac{\ln(\Delta y_{40}) - \ln(\Delta y_2)}{\ln(40) - \ln(2)}$	-1.203	-1.02	-1.009
$\frac{\ln(\Delta y_{60}) - \ln(\Delta y_2)}{\ln(60) - \ln(2)}$	-1.82	-1.029	-1.012

TABLE III. The difference of rapidity Δy from Fig.6. From these results it is evident that the dependence is close to inverse proportion.

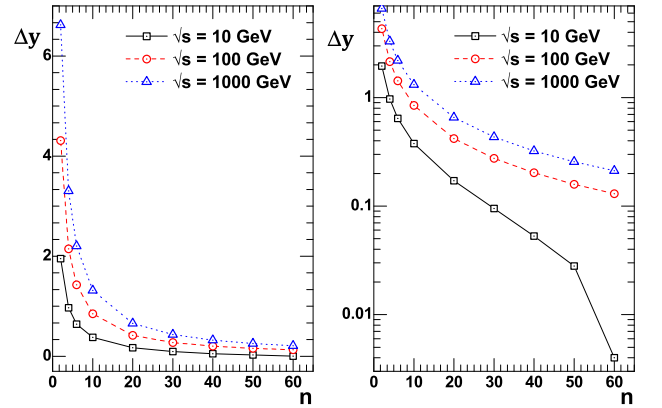


FIG. 6. Dependence of difference Δy in an arithmetic progression, which constrainedly maximizing the inelastic scattering amplitude for the different number of particles n on the “comb” at the fixed energies \sqrt{s} : 10 GeV, 100 GeV and 1000 GeV.

it is evident that, when n is small in comparison with the boundary value determined by Eq.32, this dependence is close to inversely. In particular, if we examine $\ln(\Delta y)$ as a function of $\ln(n)$, it is possible to calculate corresponding difference of an arithmetic progressions for the given energy (they are marked as $\Delta y_1, \Delta y_2, \dots, \Delta y_k$ in Fig.8). As it follows from Table.III, ratios

$$\frac{\ln(\Delta y_j) - \ln(\Delta y_2)}{\ln(n_j) - \ln(2)} \quad (33)$$

where $j = 1, 2, 3, \dots, k$ are close to (-1) , which suggests that if we fix \sqrt{s} and examine $n \ll \frac{\sqrt{s} - 2M}{m}$, that is much smaller value than the maximum allowable by law of conservation of energy for a given value \sqrt{s} , then we have $\Delta y \sim n^{-1}$.

More specific information about the dependence $\Delta y(n, \sqrt{s})$ can be obtained from analytical solution of

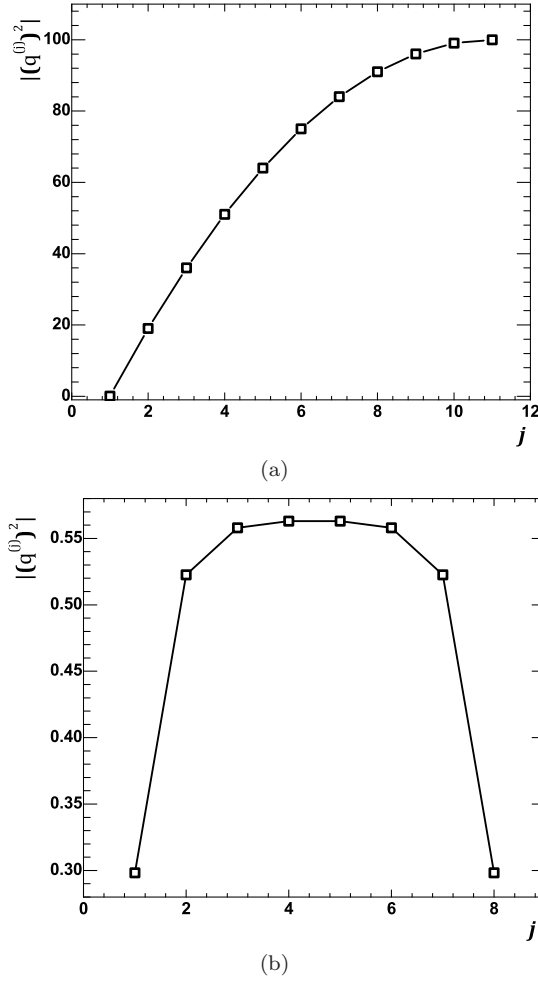


FIG. 7. The virtuality variation along “the comb”. 7(a) shows particles virtuality dependence on vertex number on diagram Fig.2, for even number of particles ($n = 20$). Only the upper half of the diagram was considered, because as it follows from symmetry relations, discussed in Section.II, virtualities at the maximum point on the lines symmetrical to symmetry axis are equal. This also evident from 7(a), which shows the virtuality variation along the whole “the comb” for odd number of particles ($n = 7$).

the constrained extremum problem for scattering amplitude, which will be considered in the next section.

However, the greatest interest is the dependence of the absolute values of virtualities on energy (i.e. the virtual particle squared four-momentums corresponding to the diagram in Fig.2, calculated at values of real particle four-momentums for which the scattering amplitude has a constrained maximum). Discussion of this problem leads us to possible mechanism of inelastic scattering cross-section growth with energy.

Let us designate the virtual particle four-momentums

according to Fig.2:

$$\begin{aligned} k^{(1)} &= P_1 - P_3, k^{(2)} = P_1 - P_3 - p_1, \dots, \\ k^{(j)} &= P_1 - P_3 - \sum_{l=1}^{j-1} p_l, \dots \end{aligned} \quad (34)$$

The numbers of four-momentums are taken in brackets to distinguish them from the four-momentum components notation. For example, notation $k^{(0)0}$ denotes zero component of contravariant four-vector $k^{(0)}$.

As was noted above, all the quantities were made dimensionless by the mass m before calculations, therefore we introduce the notation

$$q^{(j)} = \frac{k^{(j)}}{m} \quad (35)$$

At the same time the magnitude A , which is determined by Eq.4 and coincident with scattering amplitude accurate within constant, can be written in dimensionless form like:

$$A = \prod_{j=1}^{n+1} \left(1 + \left| \left(q^{(j)} \right)^2 \right| \right)^{-1} \quad (36)$$

From numerical computation we know particles four-momentums in finite state, for which function A has constrained maximum. Therefore, with help of relations Eq.34 and Eq.35 we can calculate four-momentums $q^{(j)}$ and whereupon calculate the corresponding dimensionless virtualities. Results of such calculation presented on Fig.7 and Fig.9. As it well known, that there is reference frame where the particle energy vanishes [11] for particles with negative virtuality. Such a reference frame is called the standard reference system according to terminology of [11]. Obviously that the particle momentum in the standard reference system has the smallest possible value of all inertial frames of reference, and this smallest value is defined by particle’s virtuality.

Taking into account the Heisenberg uncertainty principle, we find that the virtuality characterizes a size of the domain, in which a particle can be detected with high accuracy, if the measurements were made in the standard reference system of this particle. At the same time, the more particle’s virtuality, the smaller this size. Thus, the virtuality of particles makes it possible to judge the spatial extension of those domains, where inelastic processes take place described by the diagrams of type Fig.2. These space domains form the virtual “coats” of colliding particles, therefore these spatial extensions define typical sizes of colliding particles P_1 and P_2 , see Fig.2. From Fig.7 it is evident that virtualities increase with movement from the diagram edges to its center. This is easy to explain, because all the virtualities are negative and therefore

$$(k^{(1)})^2 = (P_1^0 - P_3^0)^2 - (P_{1\parallel} - P_{3\parallel})^2 - (\vec{P}_{3\perp})^2 < 0 \quad (37)$$

Taking into account that transversal components of momentum are equal to zero at the maximum point, we

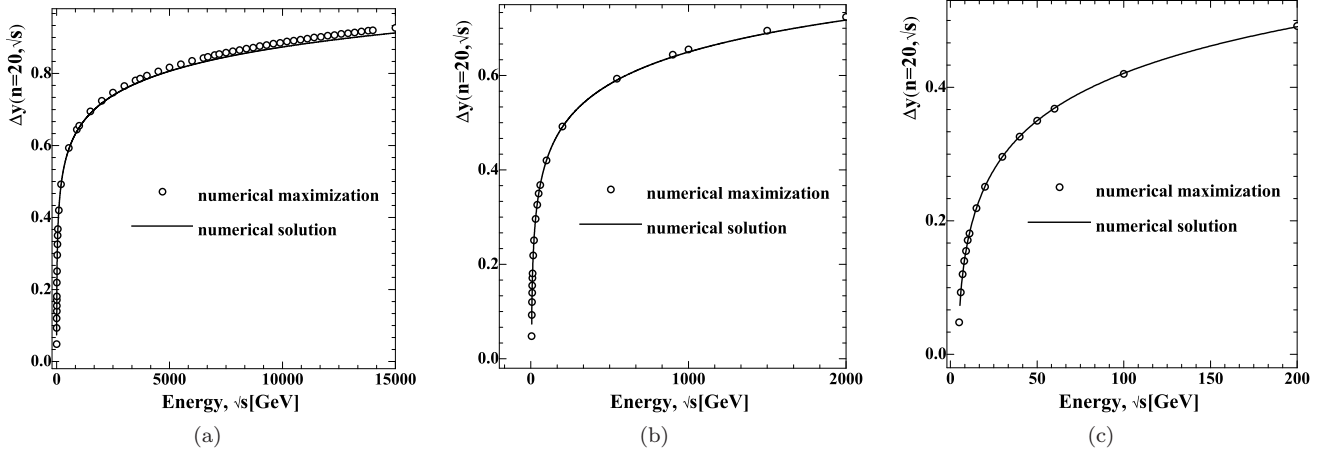


FIG. 8. Comparison of the results of the numerical solution of Eq.74 (solid line) with the results of numerical maximization (circles) of the magnitude $\Delta y(n, \sqrt{s})$ at $n = 20$ for the different energy ranges, GeV: $5 \div 16000$ (8(a)); $5 \div 2000$ (8(b)); $5 \div 200$ (8(c)). Here, it is taken into account that $\Delta y(n, \sqrt{s}) = 2y_{\frac{n}{2}}$.

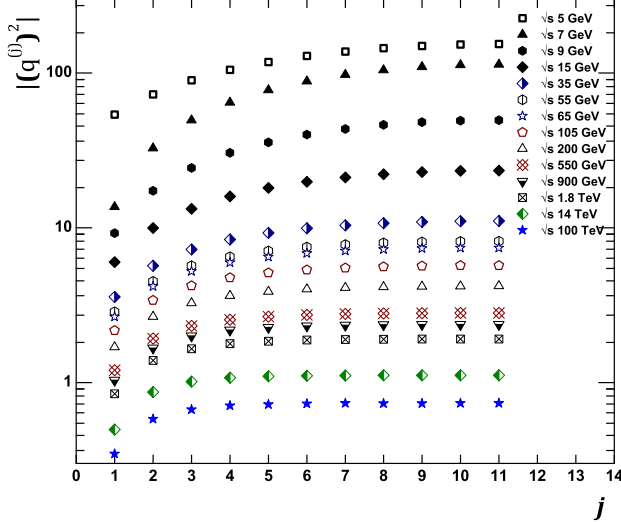


FIG. 9. Variation of the modulus of virtuality on energy for $n = 20$ at different energies.

have:

$$(P_{1\parallel} - P_{3\parallel})^2 > (P_1^0 - P_3^0) \quad (38)$$

According to the law of conservation of energy we have $P_3^0 < P_1^0$. At the same time

$$P_1^0 = \sqrt{M^2 + (P_{1\parallel})^2}$$

and

$$P_3^0 = \sqrt{M^2 + (P_{3\parallel})^2},$$

therefore $(P_{3\parallel})^2 < (P_{1\parallel})^2$. Since both these expressions are positive, we have $P_{3\parallel} < P_{1\parallel}$. Therefore due to positivity of expressions in brackets, we obtain from Eq.38:

$$P_{1\parallel} - P_{3\parallel} > P_1^0 - P_3^0 \quad (39)$$

However, when we move from $k^{(1)}$ to $k^{(2)}$, we subtract $ch(y_1)$ from the lower side $P_1^0 - P_3^0$ and $sh(y_1)$ from the higher side $P_{1\parallel} - P_{3\parallel}$. Consequently, the difference of these quantities increases, and so naturally to expect that the difference of squares, i.e., virtuality $(k^{(2)})^2$, increases too Fig.7. Turning to each subsequent virtuality, we will subtract a hyperbolic cosine of corresponding rapidity from the energy and subtract a hyperbolic sine of the same rapidity from the longitudinal momentum. The difference between the longitudinal momentum and the energy will increase, which explains the increase in the differences of their squares, i.e. virtualities.

Behavior of virtuality at the maximum point for different energies is shown in Fig.9. From the results in Fig.9 it follows that at the maximum point the virtuality monotone decreases with the energy growth. As it is evident from Eq.C6, that the decrease of the virtuality should lead to amplitude increasing with energy at the maximum point, and for reasons outlined in Section.I this should lead to increase of partial cross sections with energy \sqrt{s} growth. Such an effect is a consequence of rapidity increasing at the maximum point, and therefore in principle can not be taken into account within framework of multi-Regge kinematics [7, 9, 10, and 14] due to the fact that this dependence is neglected in the integrand of Eq.1.

Further, in the second part of our paper we will discuss the question of whether the amplitude growth can lead to growth in cross-section σ_n calculated by Laplace method and in total scattering cross-section σ_{total} .

IV. ANALYTICAL SOLUTION OF THE CONSTRAINED EXTREMUM PROBLEM FOR INELASTIC SCATTERING AMPLITUDE AT THE APPROXIMATION OF EQUAL-DENOMINATORS

We first consider in more detail the case of even number of particles n in the diagram of Fig.2. The scattering amplitude reduction $A_0(n, y_1, y_2, \dots, y_{n/2})$ defined by Eq.28 undimensioned by mass m take a form:

$$\begin{aligned} A_0(n, y_1, y_2, \dots, y_{\frac{n}{2}}) &= \\ &= \left(1 - \left(\sum_{k=1}^{\frac{n}{2}} ch(y_k) \right)^2 + (P_{1\parallel} - P_{3\parallel})^2 \right)^{-2} \\ &\times \left(1 + \left(P_{1\parallel} - P_{3\parallel} - \sum_{k=1}^{\frac{n}{2}} sh(y_k) \right)^2 \right)^{-1} \\ &\times \prod_{j=2}^{\frac{n}{2}} \left(1 - \left(\sum_{k=j}^{\frac{n}{2}} ch(y_k) \right)^2 + \left(P_{1\parallel} - P_{3\parallel} - \sum_{k=1}^{j-1} sh(y_k) \right)^2 \right)^{-2} \end{aligned} \quad (40)$$

Here $P_{1\parallel} = \sqrt{s/4 - M^2}$ and instead of \sqrt{s} and M we use their dimensionless by mass m values. Since we search for the constrained extremum, under condition of energy-momentum conservation, it is assumed that P_3 is described by Eq.26, in which again all values are undimensioned by mass m . In particular, taking into account the symmetry relation, normalization and the introduction of rapidity (see Eq.15), we obtain for E_p instead Eq.B16:

$$E_p = \sqrt{s} - 2 \sum_{k=1}^{\frac{n}{2}} ch(y_k) \quad (41)$$

For further calculations we use the following denotation

$$E = \sum_{k=1}^{\frac{n}{2}} ch(y_k) \quad \text{and} \quad \Delta P = P_{1\parallel} - P_{3\parallel} \quad (42)$$

Note that due to Eqs.26, 41 and Eq.42 quantity ΔP depends on rapidity as the composite function of E , which is denoted as $\Delta P(E)$ and the first term of Eq.40 depends on rapidity only via E .

Instead of looking for the maximum of function $A_0(n, y_1, y_2, \dots, y_{n/2})$ we can look for the maximum of its logarithm, which we define as L :

$$\begin{aligned} L &= -2 \ln \left(1 - (E)^2 + (\Delta P(E))^2 \right) \\ &- 2 \sum_{j=2}^{\frac{n}{2}} \ln \left(1 - \left(\sum_{k=j}^{\frac{n}{2}} ch(y_k) \right)^2 + \left(\Delta P(E) - \sum_{k=1}^{j-1} sh(y_k) \right)^2 \right) \\ &- \ln \left(1 + \left(\Delta P(E) - \sum_{k=1}^{\frac{n}{2}} sh(y_k) \right)^2 \right) \end{aligned} \quad (43)$$

In addition, we make following denotations:

$$\begin{aligned} Z_1 &= 1 - (E)^2 + (\Delta P(E))^2 \\ Z_j &= 1 - \left(\sum_{k=j}^{\frac{n}{2}} ch(y_k) \right)^2 + \left(\Delta P(E) - \sum_{k=1}^{j-1} sh(y_k) \right)^2 \\ Z_{\frac{n}{2}+1} &= 1 + \left(\Delta P(E) - \sum_{k=1}^{\frac{n}{2}} sh(y_k) \right)^2 \end{aligned} \quad (44)$$

where $j = 1, 2, \dots, \frac{n}{2}$

Since after taking into account Eq.B16, all variables of function $A_0(n, y_1, y_2, \dots, y_{n/2})$ and hence logarithm became independent, then the extreme point can be found under condition that partial derivatives with respect to all variables are equal to zero. The equations for the extreme point problem can be written down in a form:

$$\begin{aligned} \frac{\partial L}{\partial y_1} &= \frac{\partial L}{\partial E} sh(y_1) + 4ch(y_1) \sum_{j=2}^{\frac{n}{2}} \frac{\Delta P(E) - \sum_{k=1}^{j-1} sh(y_k)}{Z_j} \\ &+ 2ch(y_1) \frac{\Delta P(E) - \sum_{k=1}^{\frac{n}{2}} sh(y_k)}{Z_{\frac{n}{2}+1}} = 0 \end{aligned} \quad (45)$$

$$\begin{aligned} \frac{\partial L}{\partial y_l} &= \frac{\partial L}{\partial E} sh(y_l) + 4sh(y_l) \sum_{j=2}^{\frac{n}{2}} \frac{\sum_{k=j}^{\frac{n}{2}} ch(y_k)}{Z_j} \\ &+ 4ch(y_l) \sum_{j=l+1}^{\frac{n}{2}} \frac{\Delta P(E) - \sum_{k=1}^{j-1} sh(y_k)}{Z_j} \\ &+ 2ch(y_l) \frac{\Delta P(E) - \sum_{k=1}^{\frac{n}{2}} sh(y_k)}{Z_{\frac{n}{2}+1}} = 0 \end{aligned} \quad (46)$$

where $l = 2, 3, \dots, \frac{n}{2} - 1$.

$$\begin{aligned} \frac{\partial L}{\partial y_{\frac{n}{2}}} &= \frac{\partial L}{\partial E} sh(y_{\frac{n}{2}}) + 4sh(y_{\frac{n}{2}}) \sum_{j=2}^{\frac{n}{2}} \frac{\sum_{k=j}^{\frac{n}{2}} ch(y_k)}{Z_j} \\ &+ 2ch(y_{\frac{n}{2}}) \frac{\Delta P(E) - \sum_{k=1}^{\frac{n}{2}} sh(y_k)}{Z_{\frac{n}{2}+1}} = 0 \end{aligned} \quad (47)$$

Eqs.45 - 47 form the system of equations for the extreme point search. An approximate solution of this system is the purpose of this section. The simplification of this system of equations can be attained in approximation, which we call "the equal-denominators approximation".

As seen from Eq.36, the amplitude is a product of fractions whose denominators contain the expression greater

than unit. However, function $f(x) = 1/x$ slowly varying at $x > 1$, that follows from its derivative. In addition, as discussed in Section.III, virtualities increase, and hence, as it evident from Eq.38 and arguments made after this relation, the denominators increase with movement from the edges of the “comb” to its center. However, as we are looking for the maximum point, virtualities at this point should be as small as possible. Therefore, they should increase as we move from the edges of the “comb” to the center as slowly as possible. Hence, we can expect that the denominators lightly differs from each other in the desired maximum point, then for the further analysis of the system of equations at the maximum point we adopt an approximation, in which all the denominators are equal between themselves. Their approximate common value will be denoted as Z ,

$$Z_j \approx Z, \quad j = 1, 2, \dots, \frac{n}{2} + 1 \quad (48)$$

The equations for the maximum point as result of the approximation take form

$$\begin{aligned} \frac{Z}{2} \frac{\partial L}{\partial E} + 2 \frac{ch(y_1)}{sh(y_1)} \sum_{j=2}^{\frac{n}{2}} \left(\Delta P(E) - \sum_{k=1}^{j-1} sh(y_k) \right) \\ + \frac{ch(y_1)}{sh(y_1)} \left(\Delta P(E) - \sum_{k=1}^{\frac{n}{2}} sh(y_k) \right) = 0 \end{aligned} \quad (49)$$

$$\begin{aligned} \frac{Z}{2} \frac{\partial L}{\partial E} + 2 \sum_{j=2}^l \left(\sum_{k=j}^{\frac{n}{2}} ch(y_k) \right) \\ + 2 \frac{ch(y_l)}{sh(y_l)} \sum_{j=l+1}^{\frac{n}{2}} \left(\Delta P(E) - \sum_{k=1}^{j-1} sh(y_k) \right) \\ + \frac{ch(y_l)}{sh(y_l)} \left(\Delta P(E) - \sum_{k=1}^{\frac{n}{2}} sh(y_k) \right) = 0 \end{aligned} \quad (50)$$

here $l = 2, 3, \dots, \frac{n}{2} - 1$.

$$\begin{aligned} \frac{Z}{2} \frac{\partial L}{\partial E} + 2 \sum_{j=2}^{\frac{n}{2}} \left(\sum_{k=j}^{\frac{n}{2}} ch(y_k) \right) \\ + \frac{ch(y_{\frac{n}{2}})}{sh(y_{\frac{n}{2}})} \left(\Delta P(E) - \sum_{k=1}^{\frac{n}{2}} sh(y_k) \right) = 0 \end{aligned} \quad (51)$$

From approximation Eq.48, in particular, we obtain $Z_{\frac{n}{2}} \approx Z_{\frac{n}{2}+1}$. Taking into account the notation Eq.44 lead an equality:

$$\Delta P(E) - \sum_{k=1}^{\frac{n}{2}} sh(y_k) = \frac{1}{2sh(y_{n/2})} \quad (52)$$

Substituting Eq.52 to the system of equations Eq.49, Eq.50, Eq.51 we have

$$\begin{aligned} \frac{Z}{2} \frac{\partial L}{\partial E} + 2 \frac{ch(y_1)}{sh(y_1)} \sum_{j=2}^{\frac{n}{2}} \left(\frac{1}{2sh(y_{\frac{n}{2}})} + \sum_{k=j}^{\frac{n}{2}} sh(y_k) \right) \\ + \frac{ch(y_1)}{2sh(y_{\frac{n}{2}})sh(y_1)} = 0 \end{aligned} \quad (53)$$

$$\begin{aligned} \frac{Z}{2} \frac{\partial L}{\partial E} + 2 \sum_{j=2}^l \left(\sum_{k=j}^{\frac{n}{2}} ch(y_k) \right) \\ + 2 \frac{ch(y_l)}{sh(y_l)} \sum_{j=l+1}^{\frac{n}{2}} \left(\frac{1}{2sh(y_{\frac{n}{2}})} + \sum_{k=j}^{\frac{n}{2}} sh(y_k) \right) \\ + \frac{ch(y_l)}{2sh(y_{\frac{n}{2}})sh(y_l)} = 0 \end{aligned} \quad (54)$$

here $l = 2, 3, \dots, \frac{n}{2} - 1$.

$$\frac{Z}{2} \frac{\partial L}{\partial E} + 2 \sum_{j=2}^{\frac{n}{2}} \left(\sum_{k=j}^{\frac{n}{2}} ch(y_k) \right) + \frac{ch(y_{\frac{n}{2}})}{2(sh(y_{\frac{n}{2}}))^2} = 0 \quad (55)$$

Eqs.53, 54 and Eq.55 form a system of equations for search the point of the constrained maximum of inelastic scattering amplitude as approximation of equal denominators Eq.48.

To solve this system we consider Eq.54, which corresponds to $l = \frac{n}{2} - 1$:

$$\begin{aligned} \frac{Z}{2} \frac{\partial L}{\partial E} + 2 \sum_{j=2}^{\frac{n}{2}-1} \left(\sum_{k=j}^{\frac{n}{2}} ch(y_k) \right) \\ + \frac{ch(y_{\frac{n}{2}-1})}{sh(y_{\frac{n}{2}-1})} \left(\frac{3}{2sh(y_{\frac{n}{2}})} + 2sh(y_{\frac{n}{2}}) \right) = 0 \end{aligned} \quad (56)$$

Subtracting Eq.55 from Eq.56 we get

$$\begin{aligned} 2ch(y_{\frac{n}{2}}) + \frac{ch(y_{\frac{n}{2}})}{2(sh(y_{\frac{n}{2}}))^2} \\ - \frac{ch(y_{\frac{n}{2}-1})}{sh(y_{\frac{n}{2}-1})} \left(\frac{3}{2sh(y_{\frac{n}{2}})} + 2sh(y_{\frac{n}{2}}) \right) = 0 \end{aligned} \quad (57)$$

From this relation follows that

$$\begin{aligned} \text{th}(y_{\frac{n}{2}-1}) = \frac{\frac{3}{2sh(y_{\frac{n}{2}})} + 2sh(y_{\frac{n}{2}})}{2ch(y_{\frac{n}{2}}) + \frac{ch(y_{\frac{n}{2}})}{2(sh(y_{\frac{n}{2}}))^2}} = \text{th}(3y_{\frac{n}{2}}) \end{aligned} \quad (58)$$

Taking into account that a hyperbolic tangent is a monotonous function on whole real axis, from Eq.58:

$$y_{\frac{n}{2}-1} = 3y_{\frac{n}{2}} \quad (59)$$

Note that this result agrees with the numerical results shown in Fig.4 and related to it Table.II (see column y_k/y_{15} for $n = 30$). Now let us prove by induction that

$$y_{\frac{n}{2}-k} = (2k+1) y_{\frac{n}{2}}, \quad k = 1, 2, \dots, \frac{n}{2} - 1 \quad (60)$$

In the Eq.60 is already proved at $k = 1$, since it coincides

$$2 \sum_{j=l+1}^{\frac{n}{2}} \left(\sum_{k=j}^{\frac{n}{2}} ch(y_k) \right) + \frac{ch(y_{\frac{n}{2}})}{2(sh(y_{\frac{n}{2}}))^2} - 2 \frac{ch(y_l)}{sh(y_l)} \sum_{j=l+1}^{\frac{n}{2}} \left(\frac{1}{2sh(y_{\frac{n}{2}})} + \sum_{k=j}^{\frac{n}{2}} sh(y_k) \right) - \frac{ch(y_l)}{2sh(y_{\frac{n}{2}})sh(y_l)} = 0 \quad (61)$$

Note, that sums $\sum_{k=j}^{n/2} ch(y_k)$ and $\sum_{k=j}^{n/2} sh(y_k)$ under $l + 1 \leq j \leq \frac{n}{2}$ include only those y_k , that covered by induction hypothesis. Then from Eq.60 we have $\sum_{k=j}^{\frac{n}{2}} sh(y_k)$. This makes it easy to calculate the sums from Eq.61, which after transformations takes a form:

$$th(y_l) = th\left(\left(2\left(\frac{n}{2} - l\right) + 1\right) y_{\frac{n}{2}}\right) \quad (62)$$

It follows that

$$\begin{aligned} y_l &= \left(2\left(\frac{n}{2} - l\right) + 1\right) y_{\frac{n}{2}} \\ y_{\frac{n}{2}-l} &= (2l+1) y_{\frac{n}{2}} \end{aligned} \quad (63)$$

i.e., it coincides with proved Eq.60.

Thus, for diagrams with even number of particles we have shown that in the approximation of equal-denominators (see Eq.48) analytically can be reproduce results shown in the previous section of numerical computation, that rapidities at the maximum point form an arithmetic progression and that ratios of all rapidities to the minimum rapidity form the sequence of odd integers.

In order to determine the values of rapidities, for which scattering amplitude has a constrained maximum we still need to calculate the value $y_{n/2}$, used to express all rapidities. This can be done using the equal-denominators approximation Eq.48.

Calculating the sums in Eq.55 with allowance for Eq.60, we have:

$$\frac{Z}{2} \frac{\partial L}{\partial E} + \frac{ch((n-1)y_{\frac{n}{2}})}{2(sh(y_{\frac{n}{2}}))^2} = 0 \quad (64)$$

Now using relation Eq.60 for the L we calculate the derivative $\frac{\partial L}{\partial E}$. The corresponding expression will be looks like:

$$\frac{\partial L}{\partial E} = \frac{4E}{Z_1} - 4\wp \frac{\partial \Delta P(E)}{\partial E} \quad (65)$$

where

$$\wp = \frac{\Delta P(E)}{Z_1} + \sum_{j=2}^{\frac{n}{2}} \frac{\Delta P(E) - \sum_{k=1}^{j-1} sh(y_k)}{Z_j} + \frac{1}{2} \frac{\Delta P(E) - \sum_{k=1}^{\frac{n}{2}} sh(y_k)}{Z_{\frac{n}{2}+1}} \quad (66)$$

with Eq.59. Let us assume that this equation is true for $k = 1, 2, \dots, \frac{n}{2} - l - 1$ (i.e., at $y_{n/2-1}, y_{n/2-2}, \dots, y_{l+1}$) and prove that it is true at $k = \frac{n}{2} - l$ (i.e., at y_l).

Subtracting Eq.55 from Eq.54 we obtain:

Using the equal-denominators approximation Eq.48, we obtain:

$$\frac{Z}{2} \frac{\partial L}{\partial E} = 2E - 2\wp' \frac{\partial \Delta P(E)}{\partial E} \quad (67)$$

where

$$\begin{aligned} \wp' &= \Delta P(E) + \sum_{j=2}^{\frac{n}{2}} \left(\Delta P(E) - \sum_{k=1}^{j-1} sh(y_k) \right) \\ &+ \frac{1}{2} \left(\Delta P(E) - \sum_{k=1}^{\frac{n}{2}} sh(y_k) \right) \end{aligned} \quad (68)$$

Taking into account Eq.52, after transformations we get:

$$\frac{Z}{2} \frac{\partial L}{\partial E} = \frac{sh(ny_{\frac{n}{2}})}{sh(y_{\frac{n}{2}})} + \frac{sh((n+1)y_{\frac{n}{2}})}{2sh^2(y_{\frac{n}{2}})} \frac{\partial P_{3\parallel}(E)}{\partial E} = 0 \quad (69)$$

Put Eq.69 into Eq.64, we simplify obtained equation to form

$$sh((n+1)y_{\frac{n}{2}}) \frac{\partial P_{3\parallel}(E)}{\partial E} + ch((n+1)y_{\frac{n}{2}}) = 0 \quad (70)$$

Derivative $\frac{\partial P_{3\parallel}(E)}{\partial E}$ can be calculated from Eq.26 with allowance for Eq.41 and Eq.42. Based on these relations expression for $P_{3\parallel}$, which is made dimensionless by mass m , can be written as

$$P_{3\parallel} = \sqrt{(\sqrt{s}/2 - E)^2 - M^2} \quad (71)$$

where it is assumed that the values \sqrt{s} and particle masses M at the ends of the "comb" are also made dimensionless by mass m . Recall that in the numerical calculations described in previous section pion mass was set to m and proton mass - to M).

Calculating the derivative of Eq.71 and put it into Eq.70, we obtain the equation, which after simple transformations reduces to the form:

$$\frac{\sqrt{s}}{2} - E = M \cdot ch((n+1)y_{\frac{n}{2}}) \quad (72)$$

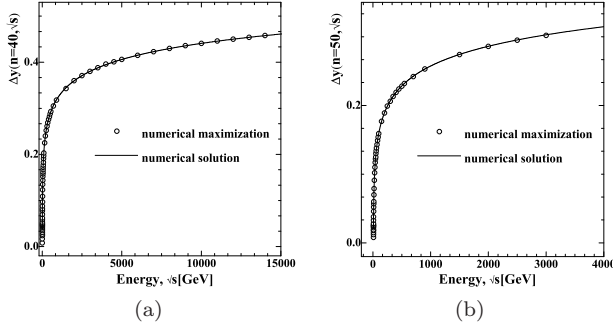


FIG. 10. The numerical solution of Eq.74 (solid line) and numerical maximization (circles) of the magnitude $\Delta y(n, \sqrt{s})$ at $n = 40$ (10(a)) and $n = 50$ (10(b)).

Note that the rapidity corresponding to momentum $P_{3\parallel}$ is equal to $(n+1)y_{n/2}$, as it follows from Eq.71 and Eq.72.

This expression would be obtained from Eq.60 if we accept $k = \frac{n}{2}$, i.e., arithmetic progression Eq.60 lengthens by one term. We can say that the rapidities of particles in the ends of the “comb” at the maximum point “continue”, as it were, an arithmetic progression, formed by the rapidities of internal particles of the “comb”. This again indicates the close relation between the equal-denominators approximation Eq.48 and the fact that rapidities at the maximum point form an arithmetic progression. In other words, the arithmetic progression formed by rapidities at the maximum point is the result of equal-denominators approximation.

It is also possible to verify permissibility of this approximation in the following way. Taking into account that

$$E = \sum_{k=1}^{\frac{n}{2}} ch(y_k) = \frac{sh(ny_{\frac{n}{2}})}{2sh(y_{\frac{n}{2}})} \quad (73)$$

(as it follows from Eq.60 and Eq.42) we get instead of Eq.72:

$$\frac{\sqrt{s}}{2} - \frac{sh(ny_{\frac{n}{2}})}{2sh(y_{\frac{n}{2}})} = M \cdot ch((n+1)y_{\frac{n}{2}}) \quad (74)$$

This equation does not admit exact analytical solution, and further we will examine an approximate solution of this equation. However, we can verify permissibility of the approximations made above, which led to Eq.74, using Mathcad 2001 (or any other computer software for engineering and scientific calculations) to solve this equation numerically for different energies \sqrt{s} and compare result with that was obtained in numerical determination of the maximum point and shown in Fig.5. The results of such comparison are shown in Fig.11 and Fig.10.

As evident from Fig.10 and Fig.11, the “exact” numerical solution of Eq.74 practically does not differ from

the results of numerical computation. This means that equal-denominators approximation Eq.48, which leads to Eq.74 is admissible approximation.

Now let us consider an approximate analytical solution of Eq.74. Note that function $sh(ny_{n/2})/2sh(y_{n/2})$ in the left-hand side of Eq.74 varies slowly at small values of $y_{n/2}$ and can be replaced for the limiting value equal to $n/2$ and $y_{n/2} \rightarrow 0$. In this approximation we obtain the following solution:

$$y_{\frac{n}{2}} = \frac{1}{n+1} \operatorname{arccosh} \left(\frac{\sqrt{s} - n}{2M} \right) \quad (75)$$

The approximate solution of Eq.75 and the results of numerical computation are presented in Fig.11, where it is evident that Eq.75 gives a somewhat overstated value in comparison with numerical computation. It is naturally, because using approximation $\frac{sh(ny_{n/2})}{2sh(y_{n/2})} \approx \frac{n}{2}$ in

Eq.74, we underestimate value of function $\frac{sh(ny_{n/2})}{2sh(y_{n/2})}$ and thereby overstated the value of the hyperbolic cosine in the right-hand side of Eq.74.

Nevertheless, as evident from Fig.11, the absolute uncertainty of approximation Eq.75 does not increase with the energy growth, as the very of $y_{n/2}$ increases, the relative error - falls. It can also be explained on the basis of Eq.74. Since $\frac{sh(ny_{n/2})}{2sh(y_{n/2})}$ becomes small in comparison with $Mch((n+1)y_{n/2})$ at sufficiently high energies \sqrt{s} (and $y_{n/2}$ accordingly) therefore, the accuracy of approximation of the function $\frac{sh(ny_{n/2})}{2sh(y_{n/2})}$ ceases to play a significant role. Neglecting $\frac{sh(ny_{n/2})}{2sh(y_{n/2})}$ in Eq.74 in comparison with $Mch((n+1)y_{n/2})$ and neglecting n in Eq.75 in comparison with \sqrt{s} , we obtain the same result. It means that approximation Eq.75 ensures the “correct” asymptotic of value $y_{n/2}$ at high \sqrt{s} .

Lets draw attention to some interesting features of Eq.75. Firstly, the approximate solution of Eq.75 has a threshold branch-point at $\sqrt{s} = n + 2M$ (dimensionless by mass m). This means that such a feature has a difference an arithmetic progression of the rapidity, for which inelastic process amplitude has maximum. The contribution of the considered inelastic processes to an imaginary part of the elastic scattering amplitude after calculation by Laplace method will be in some way expressed in terms of the difference of an arithmetic progression $\Delta y(\sqrt{s}, n)$. Therefore we can expect that noted threshold feature will be included into the imaginary part of the elastic scattering amplitude via $\Delta y(\sqrt{s}, n)$. And this feature is required by unitary condition.

Eq.75 has logarithmic asymptotic behavior at the high energies \sqrt{s} and for the case when \sqrt{s} substantially exceeding a threshold value from Eq.75 we get $\Delta y = 2y_{\frac{n}{2}}n^{-1}$, that coincides with the results of numerical computation (see Section.III).

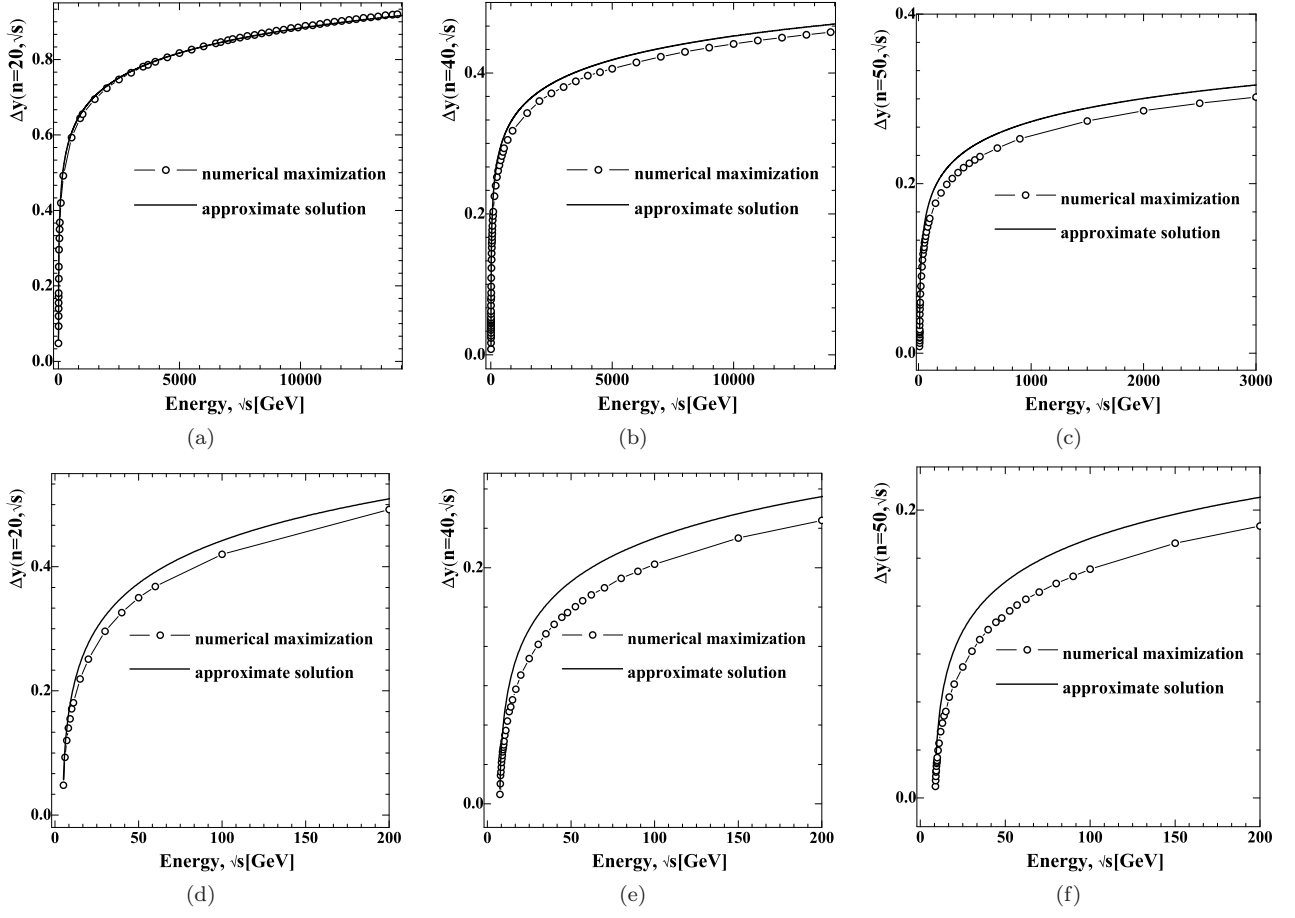


FIG. 11. Comparison of the approximate solution of Eq.74 (solid line) with the results of numerical computation (circles) at $n = 20$ (11(a)), (11(d)); $n = 40$ (11(b)), (11(e)); $n = 50$ (11(c)), (11(f)). The range of low energies close to the threshold branch point (in dimensionless form) is shown on (11(d)), (11(e)) and (11(f)). The good agreement of results shows the applicability of the approximation of equal denominators Eq.48 resulting in the Eq.72.

For the diagram in Fig.2 with odd number of particles the sequence of iterations is similar to diagrams with even number of particles, which was described above. At first we differentiate the logarithm of amplitude reduction Eq.30 with respect to all rapidities $y_1, y_2, \dots, y_{\frac{n-1}{2}}$. After that we can use the equal-denominators approximation

$$Z_1 \approx \dots \approx Z_{\frac{n-1}{2}} \approx Z_{\frac{n-1}{2}+1} = Z \quad (76)$$

From the condition of equality $Z_{\frac{n-1}{2}-1} \approx Z_{\frac{n-1}{2}}$ we get relation similar to Eq.52:

$$P_{1||} - P_{3||} - \sum_{j=1}^{\frac{n-1}{2}} sh(y_j) = \frac{ch\left(\frac{1}{2}y_{\frac{n-1}{2}}\right)}{2sh\left(\frac{1}{2}y_{\frac{n-1}{2}}\right)} \quad (77)$$

In view of Eq.77, in same way as we obtained Eq.58 from equality to zero of the derivatives of logarithm of scattering amplitude reduction with respect to $y_{\frac{n-1}{2}}$ and $y_{\frac{n-1}{2}-1}$ we get

$$y_{\frac{n-1}{2}-1} = 2y_{\frac{n-1}{2}} \quad (78)$$

This result agrees with results of the numerical calculation presented in Table.II (see column y_k/y_8 for $n = 17$). Then, just as was done above, we can prove by induction that

$$y_{\frac{n-1}{2}-(k-1)} = ky_{\frac{n-1}{2}}, \quad k = 1, 2, \dots, \frac{n-1}{2} - 1 \quad (79)$$

Thus all the rapidities, for which the considered scattering amplitude reduction has constrained maximum, can be expressed in terms of $y_{\frac{n-1}{2}}$.

Making computation similar to those that led to the relations Eqs.64-74 for this rapidity at the approximation of equal-denominators we obtain:

$$\frac{\sqrt{s}}{2} - \frac{sh\left(\frac{n}{2}y_{\frac{n-1}{2}}\right)}{2sh\left(\frac{y_{\frac{n-1}{2}}}{\frac{n}{2}}\right)} = M \cdot ch\left(\left(\frac{n-1}{2} + 1\right)y_{\frac{n-1}{2}}\right) \quad (80)$$

In an approximation similar to that, which results in Eq.75, we get

$$y_{\frac{n-1}{2}} = \frac{2}{n+1} \operatorname{arccosh}\left(\frac{\sqrt{s}-n}{2M}\right) \quad (81)$$

From Eq.81 it is evident that in the case of odd number n the rapidity difference of an arithmetic progression, for which scattering amplitude has constrained maximum, also has a threshold branch-point.

Note, that a difference of an arithmetic progression is equal to $y_{\frac{n-1}{2}}$ in case of odd n and it is equal to $2y_{\frac{n}{2}}$ in case of even n , which shows in accepted approximation that difference of an arithmetic progression $\Delta y(\sqrt{s}, n)$ is expressed by the same relation as for the even n and odd n .

The analytical results, which were obtained, allow us to trace how “works” the mechanism of virtuality reduction with the energy’s growth. In approximation of equal-denominators Eq.48 with allowance for Eq.52 the amplitude value at the maximum point (in case of even n) can be written as:

$$A^{(0),n} = \left(1 + \frac{1}{4sh^2(y_{\frac{n}{2}})}\right)^{-(n+1)} \quad (82)$$

The quantity $\frac{1}{4sh^2(y_{\frac{n}{2}})}$ included in this expression sets the characteristic value of virtuality at the maximum point of amplitude at the approximation of equal-denominators.

Taking into account increase of $y_{\frac{n}{2}}$ with energy \sqrt{s} growth, which is approximately described by Eq.75, note

$$Z_k = 1 - \left(\frac{\text{sh}\left((n-2k)\frac{\Delta y}{2}\right)}{2\text{sh}\left(\frac{\Delta y}{2}\right)}\right)^2 + \left(\sqrt{\frac{s}{4} - M^2} - M\text{sh}\left((n+1)\frac{\Delta y}{2}\right) - \frac{\text{ch}\left(n\frac{\Delta y}{2}\right) - \text{ch}\left((n-2k)\frac{\Delta y}{2}\right)}{2\text{sh}\left(\frac{\Delta y}{2}\right)}\right)^2 \quad (84)$$

Through Δy we denote (as before) the difference of arithmetic progression at the point of constrained maximum. The aim of this chapter is to obtain the approximate solution for the sum $\sum_{k=0}^{\frac{n}{2}} \ln(Z_k)$ which enters the exponent of Eq.83.

In the previous sections (see Figs.7, 9) has been shown that Feynman denominators grow if one moves from comb’s edges to its center. In other words, the maximum of Z_k values Eq.84 is $Z_{n/2}$. Furthermore, since Feynman denominators are obliged to grow while moving towards the comb’s center, the maximum of scattering amplitude is attained when the aforementioned growth is minimal. This means that the denominators at the point of maximum differ little from each other.

The results of numerical calculations enable to claim that the higher is the energy, the smaller is the difference of each Feynman denominator from the central one on the comb, with the exception of two outermost denominators (see Section.III and Figs.7, 9). This can be also shown

that virtuality at the maximum point really decreases and the maximum value of amplitude grows with energy \sqrt{s} growth.

The demonstrated results were obtained in the approximation of equal denominator Eq.48. This approximation is acceptable in order to show that the scattering amplitude has a constrained maximum point and in order to find that maximum. However, to calculate the value of the amplitude at this point, this approximation provides insufficiently accurate result, so for the next section will be calculated amplitude at the maximum point in a more accurate approximation.

V. THE APPROXIMATE CALCULATION OF THE SUM OF LOGARITHMS AT THE POINT OF CONSTRAINED MAXIMUM

Taking into account the aforementioned results (see Fig.4 and Eqs.60,79) for the calculation of constrained maximum point of multi-peripheral scattering amplitude, one gets the following representation of $A^{(0),n}$:

$$A^{(0),n} = \exp\left(-\sum_{k=0}^n \ln(Z_k)\right) = \exp\left(-2\sum_{k=0}^{\frac{n}{2}} \ln(Z_k)\right) \quad (83)$$

where

analytically (see Eq.105)

Thus, one can try to express all denominators except two outermost ones in terms of $Z_{n/2}$.

$$\ln(Z_k) = \ln\left(Z_{\frac{n}{2}}\right) + \ln\left(1 - \frac{\left(P - P_{3\parallel} - \frac{ch\left(n\frac{\Delta y}{2}\right)}{2sh\left(\frac{\Delta y}{2}\right)}\right)}{Z_{\frac{n}{2}}sh\left(\frac{\Delta y}{2}\right)} \left(1 - ch\left((n-2k)\frac{\Delta y}{2}\right)\right)\right) \quad (85)$$

Taking into account that Z_k differs little from $Z_{n/2}$, we get

$$\ln(Z_k) = \ln\left(Z_{\frac{n}{2}}\right) - \frac{\left(P - P_{3\parallel} - \frac{ch\left(n\frac{\Delta y}{2}\right)}{2sh\left(\frac{\Delta y}{2}\right)}\right)}{Z_{\frac{n}{2}}sh\left(\frac{\Delta y}{2}\right)} \left(1 - ch\left((n-2k)\frac{\Delta y}{2}\right)\right) \quad (86)$$

Substituting approximation Eq.86 into expression for scattering amplitude leads to:

$$A^{(0),n} = \frac{1}{(Z_0)^2 \left(Z_{\frac{n}{2}}\right)^{n-1}} \times \exp \left(\frac{\left(\frac{P-P_{3\parallel}}{Z_{\frac{n}{2}} \operatorname{sh}\left(\frac{y}{2}\right)} - \frac{ch\left(\frac{ny}{2}\right)}{2 \operatorname{sh}\left(\frac{y}{2}\right)} \right)}{\left(n - 1 - \frac{\operatorname{sh}\left((n-1)\frac{y}{2}\right)}{\operatorname{sh}\left(\frac{y}{2}\right)} \right)} \right) \quad (87)$$

where

$$Z_0 = 1 - \left(\sqrt{s}/2 - Mch \left((n+1) \frac{\Delta y}{2} \right) \right)^2 + \left(\sqrt{s/4 - M^2} - Msh \left((n+1) \frac{\Delta y}{2} \right) \right)^2 \quad (88)$$

$$Z_{\frac{n}{2}} = 1 + \left(\sqrt{s/4 - M^2} - Msh \left((n+1) \frac{\Delta y}{2} \right) - \frac{ch\left(n\frac{\Delta y}{2}\right)-1}{2 \operatorname{sh}\left(\frac{\Delta y}{2}\right)} \right)^2 \quad (89)$$

Relations Eqs.87-89 are expressing scattering amplitude in terms of solution Δy of transcendental equation Eq.74. Our next goal is to express scattering amplitude $A^{(0),n}$ in terms of energy \sqrt{s} , the parameter which is characterizes the scattering process. Furthermore, we can restrict ourselves to considering energies far from threshold $(\sqrt{s})_T = 2M + n$. This is due to the fact that near the threshold the behavior of partial cross-section is determined mostly by the volume of final-state particles phase space, which vanishes in the limit of $\sqrt{s} \rightarrow (\sqrt{s})_T + 0$, while $A^{(0),n}$ remains restricted with some non-zero value. Therefore, the exact value of magnitude $A^{(0),n}$ at such energies is insufficient.

VI. THE APPROXIMATE SOLUTION OF THE TRANSCENDENTAL EQUATION EXPRESSING THE DIFFERENCE OF RAPIDITY ARITHMETIC PROGRESSION AT THE POINT OF CONSTRAINED MAXIMUM OF THE SCATTERING AMPLITUDE

Consider the transcendental equation Eq.74 taking into account the fact that $\Delta y(n, \sqrt{s}) = 2y_{\frac{n}{2}}$. At energies sufficiently higher the threshold value, when is $\Delta y/2$ not small anymore, the energy of final-state protons

$$P_{30} + P_{40} = 2Mch \left((n+1) \frac{\Delta y}{2} \right) \quad (90)$$

is much higher than the pions energy $\frac{\operatorname{sh}\left(\frac{n}{2}\frac{\Delta y}{2}\right)}{\operatorname{sh}\left(\frac{1}{2}\frac{\Delta y}{2}\right)}$ which is caused with the greatness of proton mass M (in the units of pion mass) and with the fact that at not small $\Delta y/2$ one gets

$$2Mch \left((n+1) \frac{\Delta y}{2} \right) \sim \exp \left((n+1) \frac{\Delta y}{2} \right) \quad (91)$$

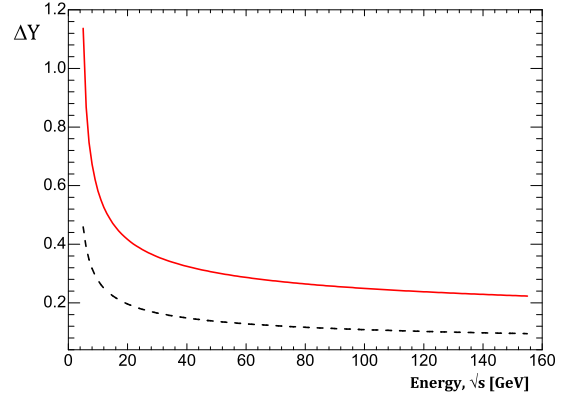


FIG. 12. The dependence of difference between initial and final-state protons rapidities on energy \sqrt{s} , calculated in the point of constrained maximum of scattering amplitude at $n = 10$ (solid line), and $n = 20$ (dash line).

while

$$\frac{\operatorname{sh}\left(\frac{n}{2}\frac{\Delta y}{2}\right)}{\operatorname{sh}\left(\frac{1}{2}\frac{\Delta y}{2}\right)} \sim \exp \left((n-1) \frac{\Delta y}{2} \right) \quad (92)$$

The fact that most of energy in c.m.s. framework is carried by secondary protons in its turn means that the rapidity of each of these protons is close on absolute value to initial proton's rapidity (let's denote it Y^*). Namely, $Y^* - (n+1)\frac{\Delta y}{2} \ll 1$ (see Fig.12). Let's enter the new variable instead of Δy

$$\Delta Y = Y^* - (n+1)\frac{\Delta y}{2} \quad (93)$$

Taking into account $\sqrt{s}/2 = Mch(Y^*)$ we'll represent Eq.74 as

$$2Msh \left(Y^* - \frac{\Delta Y}{2} \right) sh \left(\frac{\Delta Y}{2} \right) = \frac{\operatorname{sh}\left(\frac{n}{n+1}(Y^* - \Delta Y)\right)}{2 \operatorname{sh}\left(\frac{1}{n+1}(Y^* - \Delta Y)\right)} \quad (94)$$

Neglecting the small magnitude ΔY with respect to large magnitude Y^* one gets

$$sh \left(\frac{\Delta Y}{2} \right) = \frac{\operatorname{sh}\left(\frac{nY^*}{n+1}\right)}{4Msh(Y^*)sh\left(\frac{Y^*}{n+1}\right)} \quad (95)$$

Taking into account the smallness of ΔY

$$\Delta Y = \frac{\operatorname{sh}\left(\frac{nY^*}{n+1}\right)}{2Msh(Y^*)sh\left(\frac{Y^*}{n+1}\right)} \quad (96)$$

Since the arguments of hyperbolic sine and cosine functions are large

$$sh \left(\frac{\Delta Y}{2} \right) \approx \frac{1}{2M \left(\exp\left(\frac{2}{n+1}Y^*\right) - 1 \right)} \approx \frac{1}{2M \left(\left(\frac{\sqrt{s}}{M} \right)^{\frac{2}{n+1}} - 1 \right)} \quad (97)$$

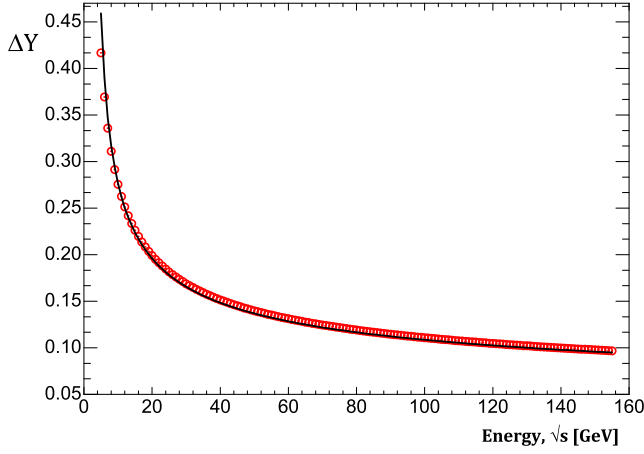


FIG. 13. The comparison of approximate solution of Eq.98 (circle) with results of numerical solution of Eq.74 with respect to magnitude ΔY (solid line) at $n = 10$.

or

$$\Delta Y \approx \frac{1}{M \left(\left(\frac{\sqrt{s}}{M} \right)^{\frac{2}{n+1}} - 1 \right)} \quad (98)$$

$$Z_i = 1 + \left(\frac{e^{(n-2i)\frac{\Delta y}{2}} - e^{-n\frac{\Delta y}{2}}}{e^{\frac{\Delta y}{2}} - e^{-\frac{\Delta y}{2}}} + M \left(e^{-Y_3} - e^{-(Y_3+dY)} \right) \right) \times \left(\sum_{l=1}^i e^{-(n+1-2l)\frac{\Delta y}{2}} + M \left(e^{-Y_3} - e^{-(Y_3+dY)} \right) \right) \quad (99)$$

where

$$Y_3 = \text{arcsh} (P_{3\parallel}/M) \quad (100)$$

If we consider the energies higher than threshold one $\sqrt{s} \ll [(\sqrt{s})_T = 2M + n]$ we can neglect the product of two small quantities in this expression. Then we get

$$Z_i \approx 1 + \frac{e^{(n-2i)\frac{\Delta y}{2}}}{e^{\frac{\Delta y}{2}} - e^{-\frac{\Delta y}{2}}} \times \left(\sum_{l=1}^i e^{-(n+1-2l)\frac{\Delta y}{2}} + M \left(e^{-Y_3} - e^{-(Y_3+dY)} \right) \right) \quad (101)$$

Then, let's consider the expression for Z_0 . Taking into account Eq.93 one can represent Eq.88 as follows

$$Z_0 = 1 + 4M^2 s h^2 \left(\frac{\Delta Y}{2} \right) \quad (102)$$

Taking into account Eq.97 we get

$$Z_0 = 1 + \left(\left(\frac{\sqrt{s}}{M} \right)^{\frac{2}{n+1}} - 1 \right)^{-2} \quad (103)$$

In order to control the applicability of made above approximations let's compare the solution of Eq.98 with the one, which can be obtained from Eq.93 substituting the “exact” solution of transcendental Eq.74 (where $\Delta y(n, \sqrt{s}) = 2y_{\frac{n}{2}}$). The result of such a comparison for $n = 10$ is depicted on Fig.13. These results enable to conclude that the entered approximations are applicable at least for rather high multiplicity of final-state particles.

Now we can pass to the approximations for other magnitudes, which enter to Eq.87, expressing the aforementioned scattering a multitude at the point of constrained maximum.

VII. THE ANALYTICAL REPRESENTATION OF FEYNMAN DENOMINATORS AT HIGH ENERGIES

Now, it is possible to analytically show the applicability of transformation Eq.86. The Feynman denominators on the comb may be represented as follows

Substituting Eq.103 into Eq.101 will result in

$$Z_i = 1 + \left(\left(\frac{\sqrt{s}}{M} \right)^{\frac{2}{n+1}} - 1 \right)^{-2} + \sum_{k=1}^i \left(\frac{M}{\sqrt{s}} \right)^{2\frac{i+1}{n+1}} \quad (104)$$

or

$$Z_{i+1} - Z_i = e^{-(i+1)\Delta y} = \left(\frac{M}{\sqrt{s}} \right)^{2\frac{i+1}{n+1}} \quad (105)$$

Namely, one can see that at high energies the difference between Feynman denominators falls exponentially. In other words, at high energies, the largest change of Feynman denominator occurs at the movement from zero (1st on the comb) to 1st (2nd on the comb) denominator. The result Eq.105 is illustrated on a Fig.14

VIII. THE ANALYTICAL EXPRESSION FOR SCATTERING AMPLITUDE DEPENDENCE ON ENERGY \sqrt{s} AT THE POINT OF CONSTRAINED MAXIMUM

In the previous analysis among the other results we derived an expression for Z_0 Eq.103. In order to verify a precision of this approximation we'll compare it with an

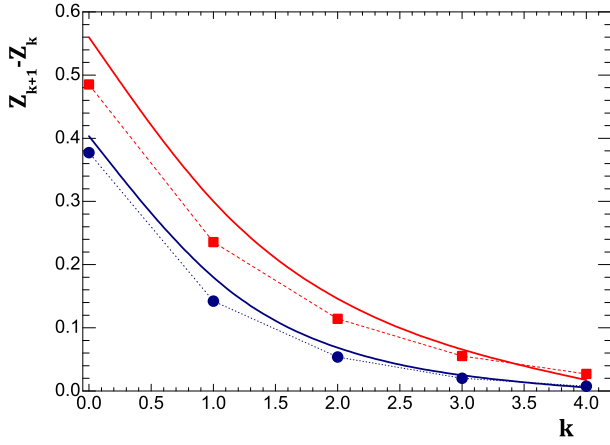


FIG. 14. The comparison for the magnitude of Feynman denominator jump on the comb at the point of constrained maximum obtained in the approximation Eq.105 (dashed lines with boxes and circles) with its exact value (red line) for $n = 10$ at $\sqrt{s} = 50$ GeV and at $\sqrt{s} = 200$ GeV (blue line).

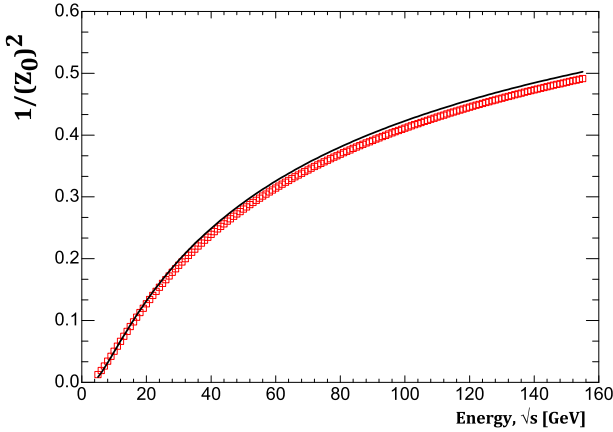


FIG. 15. The dependence of $\frac{1}{(Z_0)^2}$ on energy \sqrt{s} at $n = 10$ obtained from Eq.88 by substituting the solution of transcendental equation Eq.74 solid line; with the approximation Eq.103 boxes.

exact solution which can be obtained from Eq.88 by substituting the solution of transcendental equation Eq.94. As one can see from Fig.15 this is an adequate approximation.

Thus, we got Z_0 described analytically. Now let's get an analytical expression for two other multipliers entering to Eq.87. First we'll rewrite $Z_{n/2}$ Eq.89 in form

$$Z_{\frac{n}{2}} = 1 + \left(2M \operatorname{sh} \left(\frac{\Delta Y}{2} \right) \operatorname{ch} \left(Y^* - \frac{\Delta Y}{2} \right) - \frac{\operatorname{ch} \left(\frac{n}{n+1} (Y^* - \Delta Y) \right) - 1}{2 \operatorname{sh} \left(\frac{Y^* - \Delta Y}{n+1} \right)} \right)^2 \quad (106)$$

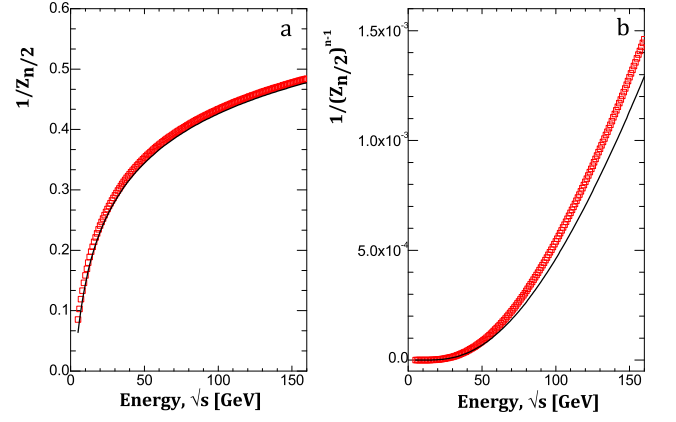


FIG. 16. The dependence of $\left(Z_{\frac{n}{2}} \right)^{-1}$ (a) and $\left(Z_{\frac{n}{2}} \right)^{-(n-1)}$ (b) on energy \sqrt{s} at $n = 10$. Solid line corresponds to Eq.89 with substituting the numerical solution of Eq.94, while dashed line refers to approximation Eq.108.

Neglecting as before ΔY with respect to Y^* and taking the common factor $\operatorname{ch}(Y^*)$ out of the brackets we get:

$$Z_{\frac{n}{2}} = 1 + s \left(\operatorname{sh} \left(\frac{\Delta Y}{2} \right) - \frac{\operatorname{ch} \left(\frac{n}{n+1} (Y^*) \right) - 1}{2M \left(\operatorname{sh} \left(\frac{n+2}{n+1} Y^* \right) - \operatorname{sh} \left(\frac{n}{n+1} Y^* \right) \right)} \right)^2 \quad (107)$$

Neglecting the small exponential summands which enters to hyperbolic sine and cosine leads us to:

$$Z_{\frac{n}{2}} \approx 1 + \left(\frac{\left(\frac{\sqrt{s}}{M} \right)^{\frac{1}{n+1}}}{\left(\frac{\sqrt{s}}{M} \right)^{\frac{2}{n+1}} - 1} \right)^2 \quad (108)$$

Again, the obtained approximation is compared with the results of numerical calculations Fig.16. Now the only thing left is to represent

$$\sqrt{\frac{s}{4} - M^2} - M \operatorname{sh} \left((n+1) \frac{\Delta y}{2} \right) - \frac{\operatorname{ch} \left(n \frac{\Delta y}{2} \right)}{2 \operatorname{sh} \left(\frac{\Delta y}{2} \right)}$$

in a more convenient form. First let's rewrite it as follows:

$$\begin{aligned} & \sqrt{\frac{s}{4} - M^2} - M \operatorname{sh} \left((n+1) \frac{\Delta y}{2} \right) - \frac{\operatorname{ch} \left(n \frac{\Delta y}{2} \right)}{2 \operatorname{sh} \left(\frac{\Delta y}{2} \right)} = \\ & = -2M \frac{\operatorname{sh} \left(Y^* + \frac{n-1}{n+1} \frac{\Delta y_1}{2} \right) - \operatorname{sh} \left(\frac{n-1}{n+1} \left(Y^* - \frac{\Delta y_1}{2} \right) \right)}{\operatorname{sh} \left(\frac{2n}{n+1} Y^* \right)} \operatorname{sh} \left(\frac{\Delta y_1}{2} \right) \end{aligned} \quad (109)$$

Performing the same trick as before, namely, neglecting ΔY with respect to Y^* and getting rid of small exponential summands we get:

$$\sqrt{\frac{s}{4} - M^2} - M \operatorname{sh} \left((n+1) \frac{\Delta y}{2} \right) - \frac{\operatorname{ch} \left(n \frac{\Delta y}{2} \right)}{2 \operatorname{sh} \left(\frac{\Delta y}{2} \right)} \approx - \frac{1}{\left(\frac{\sqrt{s}}{M} \right)} \quad (110)$$

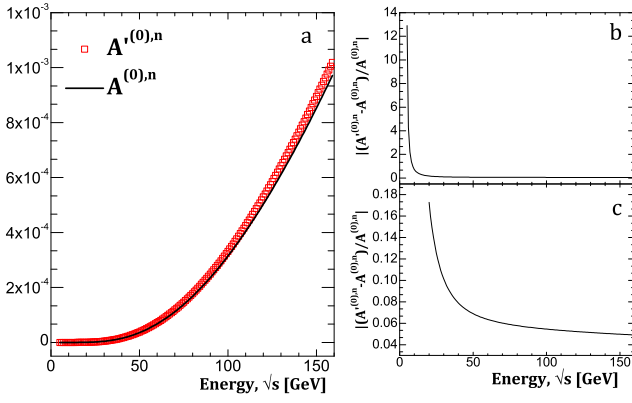


FIG. 17. The dependence of scattering amplitude in the point of constrained maximum on energy \sqrt{s} (a). Solid line corresponds to exact solution obtained from Eqs.83, 84 with a substitution of numerical solution of transcendental equation Eq.74, while dashed line represents the approximation Eqs.112; (b) the relative deviation in energy range $\sqrt{s} = 5 \div 155$ GeV; (c) the relative deviation in energy range $\sqrt{s} = 20 \div 155$ GeV.

Similarly

$$\frac{\text{sh}\left((n-1)\frac{\Delta y}{2}\right)}{\text{sh}\left(\frac{\Delta y}{2}\right)} \approx \frac{\left(\frac{\sqrt{s}}{M}\right)^{\frac{n}{n+1}}}{\left(\frac{\sqrt{s}}{M}\right)^{\frac{2}{n+1}} - 1} \quad (111)$$

Finally, let's gather all the results. Substituting Eq.103, Eq.108, Eq.110 and Eq.111 into Eq.87 we get an analytic representation of scattering amplitude at the point of constrained maximum:

$$A^{(0),n} = (1 + a(\sqrt{s}, n))^{-2} \times (1 + b(\sqrt{s}, n))^{-(n-1)} \exp(c(\sqrt{s}, n)) \quad (112)$$

where

$$\begin{aligned} a(\sqrt{s}, n) &= \left(\frac{1}{(\sqrt{s}/M)^{\frac{2}{n+1}} - 1} \right)^2 \\ b(\sqrt{s}, n) &= \left(\frac{(\sqrt{s}/M)^{\frac{1}{n+1}}}{(\sqrt{s}/M)^{\frac{2}{n+1}} - 1} \right)^2 \\ c(\sqrt{s}, n) &= 2 \left(1 - (n-1) \left(\frac{\sqrt{s}}{M} \right)^{-\frac{n}{n+1}} a^{-\frac{1}{2}}(\sqrt{s}, n) \right) \\ &\times \left(a^{-1}(\sqrt{s}, n) + \left(\frac{\sqrt{s}}{M} \right)^{\frac{2}{n+1}} \right)^{-1} \end{aligned} \quad (113)$$

The $a(\sqrt{s}, n)$ and $b(\sqrt{s}, n)$ determine the characteristic value of virtuality at the maximum point of scattering amplitude and $c(\sqrt{s}, n)$ determines the variation of virtuality along the “comb”. In other words, the following estimate takes place

$$a(\sqrt{s}, n) \leq |(q^{(j)})^2| \leq b(\sqrt{s}, n) \quad (114)$$

where $|(q^{(j)})^2|$ is the absolute value of virtuality corresponding to j -th internal line on the “comb” in the point of constrained maximum. The comparison of scattering amplitude dependence on energy \sqrt{s} obtained in analytical way with the one obtained by numerically solving Eqs.83, 84 and substituting numerical solution of Eq.74 is presented on Fig.17.

Notation $A^{(0),n}$ was introduced to distinguish the exact value of amplitude defined by the relations Eqs.83 and Eq.84 from its approximate value Eq.112. To characterize the accuracy of approximation Eq.112 was introduced a relative deviation (see Fig.17b and Fig.17c):

$$\varepsilon = \left| \frac{A'^{(0),n} - A^{(0),n}}{A^{(0),n}} \right| \quad (115)$$

IX. DISCUSSION AND CONCLUSIONS

The main results and conclusion of this paper is that the multi-peripheral scattering amplitude indeed has a point of constrained maximum under conditions of the energy-momentum conservation law. This leads to the fact that the principal contribution to the multi-dimensional integrals, which representing the inelastic scattering cross-section with the production of a given number of particles, makes a small neighborhood of the maximum point.

Analyzing properties of the maximum point leads to some differences of the physical picture of the multi-peripheral processes from ones, which leads to the basic formulas of Reggeon theory [5, 8, and 15]. In particular, the rapidities of secondary particles at the maximum point are arranged and are equidistant from each other, as assumed in the justification of Reggeon formulas. At the same time in the presented model the distance between the adjacent rapidities (i.e., difference of an arithmetic progression) depends on energy \sqrt{s} and on number of particles n (see Eq.75 and Eq.81), but not a constant value close to unity, as it accepted, for instance, in [5] and [8]. The assumption that the interval between adjacent rapidities does not depend on energy plays an important role for the ground of power dependence of the imaginary part of elastic scattering amplitude on Lorentz-invariant s , that results in the Regge pole.

As it follows from Eq.114 energy term included in both sides is useful to rewrite it in this form

$$\left(\frac{\sqrt{s}}{M} \right)^{\frac{1}{n+1}} = \exp \left(\frac{1}{n+1} \ln \left(\frac{\sqrt{s}}{M} \right) \right) \quad (116)$$

It is obvious that the growth of exponent with energy \sqrt{s} is much weaker than the corresponding decrease with the growth of number of particles n . Thus, one can see that at not very small n the value of $(\sqrt{s}/M)^{\frac{1}{n+1}} \sim 1$ even at high energies ($\sqrt{s} \gg M$). As the result, the difference of energy and longitudinal momentum squares is

at least not negligible with respect to transverse momentum for each virtuality on the “comb”. This result comes in contradiction with the statement that virtualities can be reduced to transverse momentum squares, which is usually claimed in the standard approach [2–5, 7–10].

Taking into account the growth of $(\sqrt{s}/M)^{\frac{2}{n+1}}$ with energy \sqrt{s} growth, we see that virtuality at the maximum point really decreases and the maximum value of amplitude grows with the growth of energy \sqrt{s} . Note also that at not very small n the $(\sqrt{s}/M)^{\frac{2}{n+1}}$ is close to unity at rather wide energy range which results in the much steeper growth than the one which is attained in Regge-based theories [1 and 3] and described by factor of $\ln^{n-2}(\sqrt{s}/M)$. Moreover, the higher n , the wider is the energy range. Thus the asymptotic behavior for different n is reached at different \sqrt{s} which enables to doubt the validity of the asymptotic formulas of multi-Regge kinematics.

In addition, as it follows from an examination of multi-peripheral diagrams in [3] and [5], Reggeon formulas are derived in case of total disregard to the dependence of the integrand for the cross section of production a certain number of particles on the rapidity of these particles. In such an approach a cross-section is defined by the value of rapidity phase volume. It is also well evident from the comparison of dependence of a set number particle production on \sqrt{s} with the calculation of so-called volume of “transversal-truncated phase space” [2].

Obviously, that at the described above approach the dependence of scattering amplitude on rapidity is substantial, because just this dependence determines the value of scattering amplitude in the neighborhood of the most probable configuration of momentums.

Existence of the constrained maximum point in multi-peripheral scattering amplitude and properties of this maximum allow us to apply this information for the calculation of inelastic scattering cross-section. This is the main purpose of our next paper.

Appendix A: The proof of spatial similarity of virtual particle four-momentums in the diagram of Fig.2

We carry out the proof by “contradiction”. Suppose that any of the four-momentums of virtual particles, for example, $P_1 - P_3 - p_1 - p_2 - \dots - p_k$ is time-like. Note that this four-momentum must be equal to $P_4 - P_2 + p_n + p_{n-1} + \dots + p_{k+1}$ by virtue of the law of energy-momentum conservation.

We assume that the time component of time-like four-momentum (energy) can not vanish in any inertial system. This means that the sign of the time component of such four-momentum is the Lorentz-invariant quantity, i.e., can not be changed when we move from one inertial system to another.

If we assume that the sign of the time components of four-momentum $P_1 - P_3 - p_1 - p_2 - \dots - p_k$ (or four-vector

$P_4 - P_2 + p_n + p_{n-1} + \dots + p_{k+1}$) is positive, the following inequalities must be simultaneously satisfied in all the inertial systems:

$$(P_1)^0 - (P_3)^0 - (p_1)^0 - \dots - (p_{k-1})^0 - (p_k)^0 > 0 \quad (\text{A1})$$

$$(P_4)^0 - (P_2)^0 + (p_n)^0 + (p_{n-1})^0 + \dots + (p_{k+1})^0 > 0 \quad (\text{A2})$$

Given that both inequalities include the energy components of the energy-momentum four-vectors of real particles, satisfying to the mass shell conditions, we can rewrite them as

$$\begin{aligned} & \sqrt{M^2 + (\vec{P}_1)^2} - \sqrt{M^2 + (\vec{P}_3)^2} - \sqrt{m^2 + (\vec{p}_1)^2} \\ & \dots - \sqrt{m^2 + (\vec{p}_{k-1})^2} - \sqrt{m^2 + (\vec{p}_k)^2} > 0 \end{aligned} \quad (\text{A3})$$

$$\begin{aligned} & \sqrt{M^2 + (\vec{P}_4)^2} - \sqrt{M^2 + (\vec{P}_2)^2} + \sqrt{m^2 + (\vec{p}_n)^2} \\ & + \sqrt{m^2 + (\vec{p}_{n-1})^2} + \dots + \sqrt{m^2 + (\vec{p}_{k+1})^2} > 0 \end{aligned} \quad (\text{A4})$$

Note that first of these inequalities can not take place in the rest frame of particle P_1 because

$$\begin{aligned} & \sqrt{M^2} - \sqrt{M^2 + (\vec{P}_3)^2} - \sqrt{m^2 + (\vec{p}_1)^2} \\ & \dots - \sqrt{m^2 + (\vec{p}_{k-1})^2} - \sqrt{m^2 + (\vec{p}_k)^2} < 0 \end{aligned} \quad (\text{A5})$$

If we assume that the time component of considered four-vector has a negative sign, then we obtain that in all inertial systems the following inequalities must be simultaneously satisfied:

$$\begin{aligned} & \sqrt{M^2 + (\vec{P}_1)^2} - \sqrt{M^2 + (\vec{P}_3)^2} - \sqrt{m^2 + (\vec{p}_1)^2} \\ & \dots - \sqrt{m^2 + (\vec{p}_{k-1})^2} - \sqrt{m^2 + (\vec{p}_k)^2} < 0 \end{aligned} \quad (\text{A6})$$

$$\begin{aligned} & \sqrt{M^2 + (\vec{P}_4)^2} - \sqrt{M^2 + (\vec{P}_2)^2} + \sqrt{m^2 + (\vec{p}_n)^2} \\ & + \sqrt{m^2 + (\vec{p}_{n-1})^2} + \dots + \sqrt{m^2 + (\vec{p}_{k+1})^2} < 0 \end{aligned} \quad (\text{A7})$$

However, second of these inequalities can not take place in the rest frame of particle P_2 .

Thus, we can satisfy of energy-momentum conservation law in all inertial systems only in case, if the time component of considered four-vector changes a sign when moving from one reference frame to other. However in this case this four-vector can not be time-like. Because presented argumentation is applicable to any of virtual four-momentums in the diagram Fig.2, they must all be space-like. Quod erat demonstrandum.

Appendix B: The proof of Eq.17 from Section.II

Using function $A_{\parallel}(n, y_1, y_2, \dots, y_n)$ defined by Eq.12, let us examine function $A'_{\parallel}(n, y_1, y_2, \dots, y_n)$, which is defined by relation:

$$\begin{aligned} A'_{\parallel} & (n, y_1, y_2, \dots, y_{\frac{n}{2}-1}, y_{\frac{n}{2}}, y_{\frac{n}{2}+1}, \dots, y_{n-1}, y_n) \\ & = A_{\parallel}(n, -y_n, -y_{n-1}, \dots, -y_{\frac{n}{2}}, \dots, -y_2, -y_1) \end{aligned} \quad (\text{B1})$$

The expression

$$A'_{\parallel}(n, y_1, y_2, \dots, y_n) \quad (\text{B2})$$

we would obtain if we were choose the direction of longitudinal momentum $P_{2\parallel}$ as the positive direction of collision axis and interchange the four-momentums of particles in the diagram, arranged symmetrically about the axis in Fig.3 (numeration of the diagram vertices corresponds to Fig.2).

In order to write function Eq.B2 in explicit form, we will at first rewrite it in following way:

$$\begin{aligned} A_{\parallel} & = \left(m - \left(\frac{\sqrt{s}}{2} - P_{30} \right)^2 + (S_k)^2 \right)^{-1} \\ & \times \prod_{k=1}^{n-1} \left(m - (E_k)^2 + \left(S_k - m \sum_{l=1}^k sh(y_l) \right)^2 \right)^{-1} \\ & \times \left(m - (E_n)^2 + \left(S_k - m \sum_{l=1}^n sh(y_l) \right)^2 \right)^{-1} \end{aligned} \quad (\text{B3})$$

where

$$S_k = \sqrt{s/4 - M^2} - P_{3\parallel} \quad (\text{B4})$$

$$E_k = \sqrt{s}/2 - \left(P_{30} + m \sum_{l=1}^k ch(y_l) \right) \quad (\text{B5})$$

$$E_n = \sqrt{s}/2 - \left(P_{30} + m \sum_{l=1}^n ch(y_l) \right) \quad (\text{B6})$$

Moreover, as

$$P_{3\parallel}(y_1, y_2, \dots, y_n) = \frac{1}{2}P_{\parallel p} + \frac{1}{2}E_p \sqrt{1 - \frac{4M^2}{E_p^2 - P_{\parallel p}^2}} \quad (\text{B7})$$

with

$$E_p = E_p(y_1, y_2, \dots, y_n) = \frac{\sqrt{s}}{2} - m \sum_{k=1}^n ch(y_k) \quad (\text{B8})$$

$$P_{\parallel p} = P_{\parallel p}(y_1, y_2, \dots, y_n) = -m \sum_{k=1}^n sh(y_k) \quad (\text{B9})$$

then we obtain:

$$\begin{aligned} P_{3\parallel}(-y_n, \dots, -y_2, -y_1) & = \\ -\frac{1}{2}P_{\parallel p} + \frac{1}{2}E_p \sqrt{1 - \frac{4M^2}{E_p^2 - P_{\parallel p}^2}} & = -P_{4\parallel}(y_1, y_2, \dots, y_n) \end{aligned} \quad (\text{B10})$$

and accordingly

$$\begin{aligned} & P_{30}(-y_n, \dots, -y_2, -y_1) \\ & = \sqrt{m^2 + (-P_{4\parallel}(y_1, y_2, \dots, y_n))^2} = P_{40}(y_1, y_2, \dots, y_n) \end{aligned} \quad (\text{B11})$$

With this we get

$$\begin{aligned} A'_{\parallel} & = \left(m - \left(\frac{\sqrt{s}}{2} - P_{40} \right)^2 + (S'_k)^2 \right)^{-1} \\ & \times \prod_{k=1}^{n-1} \left(m - (E'_k)^2 + \left(S'_k + m \sum_{i=n}^{n-k+1} sh(y_i) \right)^2 \right)^{-1} \\ & \times \left(m - (E'_n)^2 + \left(S'_k + m \sum_{i=1}^n sh(y_i) \right)^2 \right)^{-1} \end{aligned} \quad (\text{B12})$$

where

$$S'_k = \sqrt{s/4 - M^2} + P_{4\parallel} \quad (\text{B13})$$

$$E'_k = \sqrt{s}/2 - \left(P_{40} + m \sum_{i=1}^{n-k+1} ch(y_i) \right) \quad (\text{B14})$$

$$E'_n = \sqrt{s}/2 - \left(P_{40} + m \sum_{i=1}^n ch(y_i) \right) \quad (\text{B15})$$

Or in more convenient form expression Eq.B12 looks like:

$$\begin{aligned} A'_{\parallel} & = \left(m - \left(\frac{\sqrt{s}}{2} - P_{40} \right)^2 + (S'_k)^2 \right)^{-1} \\ & \times \prod_{k=1}^{n-1} \left(m - (E''_k)^2 + \left(S'_k + m \sum_{i=n-k+1}^n sh(y_i) \right)^2 \right)^{-1} \\ & \times \left(m - (E''_n)^2 + \left(S'_k + m \sum_{i=1}^n sh(y_i) \right)^2 \right)^{-1} \end{aligned} \quad (\text{B16})$$

where

$$E''_k = \sqrt{s}/2 - \left(P_{40} + m \sum_{i=n-k+1}^n ch(y_i) \right) \quad (\text{B17})$$

$$E''_n = \sqrt{s}/2 - \left(P_{40} + m \sum_{i=1}^n ch(y_i) \right) \quad (\text{B18})$$

We take into account that amplitude depends on the rapidity, which satisfy the conservation laws of energy and longitudinal momentum components:

$$\begin{aligned} \sqrt{s} - P_{30} - P_{40} - m \sum_{i=1}^n ch(y_i) & = 0 \\ P_{3\parallel} + P_{4\parallel} + m \sum_{i=1}^n sh(y_i) & = 0 \end{aligned} \quad (\text{B19})$$

From the conservation of the longitudinal component of momentum, we obtain

$$P_{3\parallel} + m \sum_{i=1}^{n-k} sh(y_i) = -P_{4\parallel} - m \sum_{i=n-k+1}^n sh(y_i); \quad k < n$$

$$P_{3\parallel} + m \sum_{i=1}^n sh(y_i) = -P_{4\parallel}; \quad k = n \quad (\text{B20})$$

From the energy conservation law we have

$$\sqrt{s}/2 - P_{40} = - \left(\sqrt{s}/2 - P_{30} - m \sum_{i=1}^n ch(y_i) \right) \quad (\text{B21})$$

and

$$\begin{aligned} & \sqrt{s}/2 - \left(P_{40} + m \sum_{i=n-k+1}^n ch(y_i) \right) \\ &= - \left(\sqrt{s}/2 - P_{30} - m \sum_{i=1}^{n-k} ch(y_i) \right) \end{aligned} \quad (\text{B22})$$

Substituting Eq.B22 to Eq.B16 we obtain:

$$\begin{aligned} A'_{\parallel} &= \left(m - \left(\frac{\sqrt{s}}{2} - P_{30} \right)^2 + (S''_k)^2 \right)^{-1} \\ &\times \prod_{k=1}^{n-1} \left(m - (E''_k)^2 + \left(S''_k - m \sum_{i=1}^{n-k} sh(y_i) \right)^2 \right)^{-1} \\ &\times \left(m - (E''_n)^2 + \left(S''_k - m \sum_{i=1}^n sh(y_i) \right)^2 \right)^{-1} \end{aligned} \quad (\text{B23})$$

where

$$S''_k = \sqrt{s/4 - M^2} - P_{3\parallel} \quad (\text{B24})$$

$$E''_n = \sqrt{s}/2 - \left(P_{30} - m \sum_{i=1}^n ch(y_i) \right) \quad (\text{B25})$$

$$E''_k = \sqrt{s}/2 - \left(P_{30} + m \sum_{i=1}^{n-k} ch(y_i) \right) \quad (\text{B26})$$

Replacing index $k = n - j$ in product included in the expression for amplitude, we obtain the expression coincident with Eq.12 (taking into account Eq.15)

$$A_{\parallel}(n, y_1, y_2, \dots, y_n) = A'_{\parallel}(n, y_1, y_2, \dots, y_n) \quad (\text{B27})$$

Taking into account Eq.B1, we obtain the required relation Eq.17:

$$\begin{aligned} & A_{\parallel}(n, y_1, y_2, \dots, y_{\frac{n}{2}}, y_{\frac{n}{2}+1}, \dots, y_n) \\ &= A_{\parallel}(n, -y_n, -y_{n-1}, \dots, -y_{\frac{n}{2}+1}, -y_{\frac{n}{2}}, \dots, -y_1) \end{aligned} \quad (\text{B28})$$

Appendix C: Calculation of the energies of the virtual lines that intersect with the axis of symmetry of the diagrams in Fig.3

Let us examine at first the case of an even number of particles. The law of conservation of energy in c.m.s has a form:

$$\sqrt{s} = \sum_{k=1}^n m \cdot ch(y_k) + \sqrt{M^2 + (P_{3\parallel})^2} + \sqrt{M^2 + (P_{4\parallel})^2} \quad (\text{C1})$$

Since constrained maximum of the scattering amplitude gives a symmetric configuration of $y_{n-k+1} = -y_k$, $k = 1, 2, \dots, \frac{n}{2}$ and $P_{4\parallel} = -P_{3\parallel}$ (that follows from Eq.26), then at the maximum point we get:

$$2 \sum_{k=1}^{\frac{n}{2}} m \cdot ch(y_k) + 2\sqrt{M^2 + (P_{3\parallel})^2} = \sqrt{s} \quad (\text{C2})$$

hence

$$\frac{\sqrt{s}}{2} - \sqrt{M^2 + (P_{3\parallel})^2} - \sum_{k=1}^{\frac{n}{2}} m \cdot ch(y_k) = 0 \quad (\text{C3})$$

However expression Eq.C3 corresponds to the energy transferred through the central link of the diagram between vertices with numbers of $\frac{n}{2}$ and $\frac{n}{2}+1$ (Fig.2, Fig.3), therefore this energy is equal to zero at the maximum point.

Now let ladder has odd number of particles n . Writing the law of conservation energy, we select in the sum of pion energies the term corresponding to the central particle in the diagram:

$$\begin{aligned} & \sum_{k=1}^{\frac{n-1}{2}} m \cdot ch(y_k) + m \cdot ch\left(y_{\frac{n-1}{2}+1}\right) + \sum_{k=\frac{n-1}{2}+2}^n m \cdot ch(y_k) \\ &+ \sqrt{M^2 + (P_{3\parallel})^2} \sqrt{M^2 + (P_{4\parallel})^2} = \sqrt{s} \end{aligned} \quad (\text{C4})$$

The maximum of inelastic scattering amplitude is reached at the symmetric configuration. It is characterized by the fact that the central particle has zero rapidity and the particles located symmetrically about the center particle have mutually oppositely rapidities, therefore

$$2 \sum_{k=1}^{\frac{n-1}{2}} m \cdot ch(y_k) + m + 2\sqrt{M^2 + (P_{3\parallel})^2} = \sqrt{s} \quad (\text{C5})$$

It follows that

$$\frac{\sqrt{s}}{2} - \sqrt{M^2 + (P_{3\parallel})^2} - \sum_{k=1}^{\frac{n-1}{2}} m \cdot ch(y_k) = \frac{m}{2} \quad (\text{C6})$$

Thus, the energy, which flows between $\frac{n-1}{2}$ -th and $\frac{n-1}{2} + 1$ -th particles at the most probable configuration, is equal to $\frac{m}{2}$. As $\frac{n-1}{2} + 1$ -th particle takes away energy m (which has zero rapidity at the maximum point), then the following link in the diagram will be transferred energy $\frac{-m}{2}$.

REFERENCES

- ¹D. Amati, A. Stanghellini, and S. Fubini, “Theory of high-energy scattering and multiple production,” *Il Nuovo Cimento* (1955-1965) **26**, 896–954 (1962), 10.1007/BF02781901.
- ²E. Byckling and K. Kajantie, *Particle kinematics* (Wiley, London, 1973).
- ³P. D. B. Collins, *An introduction to Regge theory and high energy physics*, Cambridge monographs on mathematical physics (Cambridge Univ. Press, Cambridge, 1977).
- ⁴E. Kuraev, L. Lipatov, and V. Fadin, “Multi reggeon processes in the yang-mills theory,” *Sov. Phys. JETP*. **44**, 443–450 (1976).
- ⁵Y. Nikitin and I. Rozental, *Theory of multiparticle production processes*, Stud. High Energ. Phys. (Harwood, Chur, 1988) transl. from the Russian.
- ⁶E. M. Levin and M. G. Ryskin, “Multiplicity distribution in the multiperipheral model,” *Yad. Fiz.* **19**, 669–681 (1974).
- ⁷E. Levin and M. Ryskin., *Results of Regge scheme development and experiment*, Vol. 158 (Uspekhi Fizicheskikh Nauk, 1989).
- ⁸K. Ter-Martirosyan, *Results of Regge scheme development and experiment* (MIPHI, Moscow, 1975).
- ⁹M. G. Kozlov, A. V. Reznichenko, and V. S. Fadin, “Quantum chromodynamics at high energies,” *Vestnik NSU* **2**, 3–31 (2007).
- ¹⁰L. N. Lipatov, “Bjorken and regge asymptotics of scattering amplitudes in qcd and in supersymmetric gauge models,” *Uspekhi Fizicheskikh Nauk* **178**, 663–668 (2008).
- ¹¹N. G. De Bruijn, *Asymptotic methods in analysis; 1st ed.*, Bibl. Matematica (North-Holland, Amsterdam, 1958).
- ¹²Brent and Maxfield, *Essential Mathcad for Engineering, Science, and Math*.
- ¹³“Mathcad official website,” <http://www.ptc.com/appserver/mkt/products/home.jsp?k=3901>.
- ¹⁴L. N. Lipatov, “Integrability properties of high energy dynamics in multi-color qcd,” *Uspekhi Fizicheskikh Nauk* **174**, 337–352 (2004).
- ¹⁵M. Baker and K. A. Ter-Martirosyan, “Gribov’s reggeon calculus: Its physical basis and implications,” *Physics Reports* **28**, 1 – 143 (1976).